

Generalized Mesons in Dense QCD

Mannque Rho^{a,b1}, Edward Shuryak^{b2}, Andreas Wirzba^{c3} and Ismail Zahed^{b4}

^a *Service de Physique Théorique, CE Saclay, 91191 Gif-sur-Yvette, France*

^b *Department of Physics and Astronomy, SUNY-Stony-Brook, NY 11794, U. S. A.*

^c *FZ Jülich, Institut für Kernphysik (Theorie), D-52425 Jülich, Germany*

Abstract

QCD superconductors in the color-flavor-locked (CFL) phase support excitations (generalized mesons) that can be described as pairs of particles or holes (rather than particle-hole) around a gapped Fermi surface. In weak coupling and to leading logarithm accuracy the scalar and pseudoscalar excitations are massless and the vector and axial-vector excitations are massive and degenerate. The massless scalar excitations are combined with the longitudinal gluons leading to the Meissner effect in the CFL phase. The mass of the composite vector excitations is close to twice the gap in weak coupling, but goes asymptotically to zero with increasing coupling thereby realizing Georgi's vector limit in cold and dense matter. We discuss the possible mixing of the composite scalar and vector excitations with the gluons, their possible coupling to the modified photons and their decay into light pseudoscalars in the CFL phase. The issue of hidden gauge-symmetry in the QCD superconductor is critically examined. The physical implications of our results on soft dilepton and neutrino emission in cold and dense matter are briefly discussed.

¹E-mail: rho@spht.saclay.cea.fr

²E-mail: shuryak@nuclear.physics.sunysb.edu

³E-mail: a.wirzba@fz-juelich.de

⁴E-mail: zahed@zahed.physics.sunysb.edu

1. Introduction

QCD at large quark density has been discussed in the literature since the late seventies [1, 2], but it has generated an intense activity especially in the last three years [3, 4, 5], in light of the fact that the ground state may exhibit a robust superconducting phase, with novel and nonperturbative phenomena. At high quark chemical potential, these phenomena are accessible by weak coupling analysis. The QCD superconductor for a number of flavors $N_f \geq 3$ and a set of degenerate quark masses, breaks color and flavor symmetry spontaneously, with the excitation of light Goldstone modes.

Some properties of these light excitations that we may call “superpions” ^{#1} have been addressed recently using effective Lagrangians [6, 7, 8]. In the latter the finite size of the pairs is usually ignored, allowing for a description in terms of point-like excitations as originally suggested in [6]. However, in weak coupling, this approximation need not be invoked since a full analysis with finite size taken into account is feasible to a leading-logarithm accuracy. A direct analysis of the light Goldstone modes in weak coupling *without* using the zero-size approximation, has been performed recently [9]. It allows a microscopic calculation of the pion form factor, decay constant and mass in leading logarithm approximation in the color-flavor-locked (CFL) phase. The self-generated form factors provide a natural cutoff to regulate the effective calculations at the Fermi surface.

In this paper, we will pursue the microscopic analysis for the generalized scalar, vector and axial-vector mesons viewed as composites of pairs of quasiparticles or quasiholes in the CFL phase. Throughout, we will only discuss the octet phase and its associated set of generalized mesons. The axial $SU(3)$ singlet is still expected to be split by the color-flavor triangle-anomaly [6] present in the CFL phase. This issue will be addressed elsewhere. In section 2, we discuss the general features of the QCD superconductor in the CFL phase. In section 3, we show that in the CFL phase both the pseudoscalar and scalar excitations are massless. The former are true Goldstone modes, while the latter are would-be Goldstone modes that combine with the longitudinal gluons as discussed in section 4. In section 5, we show that bound vector excitations of particles or holes exist in the CFL phase, and derive an explicit relation for their form factor and mass. In section 6, we discuss their coupling to currents. To leading logarithm accuracy the octet of vectors are degenerate with the octet of axial-vectors, and decouple from the Noether currents. In section 7, we show that the composite vectors do not decay to pions in leading logarithm accuracy, contrary to their analogues in the QCD vacuum. In section 8, we show that the composite vectors decouple from the gluons in the CFL phase as well. In section 9, we show that issues such as vector dominance and gauge universality do not *immediately* apply to the generalized mesons of finite size. A hidden local symmetry can be revealed only for zero size pairs, which may not

^{#1}We will use the phrases “superpion”, “supervector” etc. for denoting the generalized mesons in the zero-size approximation which is behind the “superqualiton” point of view of [6].

constitute a good approximation for magnetically bound pairs. Our conclusions are given in section 10. Some of the calculations are relegated to the Appendix.

2. QCD Superconductor in the CFL Phase

As shown in [3], in the CFL phase the quarks have a nonzero gap. Their propagation is given in the Nambu-Gorkov formalism by a matrix written in terms of the two-component Nambu-Gorkov field $\Psi = (\psi, \psi_C)$, where ψ refers to quarks and $\psi_C(q) = C\bar{\psi}^T(-q)$ to charge conjugated quarks, respectively ^{#2}. For large μ , the antiparticles decouple, and the propagator $\mathbf{S}(q)$ in the chiral limit reads [10, 11]

$$\mathbf{S}(q) \approx \begin{pmatrix} \gamma^0(q_0 + q_{||})\Lambda^-(\mathbf{q}) & -\mathbf{M}^\dagger G^*(q)\Lambda^+(\mathbf{q}) \\ \mathbf{M}G(q)\Lambda^-(\mathbf{q}) & \gamma^0(q_0 - q_{||})\Lambda^+(\mathbf{q}) \end{pmatrix} \frac{1}{q_0^2 - \epsilon_q^2}, \quad (1)$$

where $q_{||} \approx (|\mathbf{q}| - \mu)$ is the particle or hole momentum in the direction of the Fermi momentum, such that the particle/hole energies read $\epsilon_q \approx \mp \sqrt{q_{||}^2 + |G(q)|^2}$ in terms of the gap function $G(q)$. The operators $\Lambda^\pm(\mathbf{q}) = \frac{1}{2}(1 \pm \boldsymbol{\alpha} \cdot \hat{\mathbf{q}})$ are the positive and negative energy projectors ^{#3}. In the CFL phase $\mathbf{M} = \epsilon_f^a \epsilon_c^a \gamma_5 = \mathbf{M}^\dagger$ with two antisymmetric tensors $(\epsilon^a)^{bc} = \epsilon^{abc}$, $a, b, c \in \{1, 2, 3\}$, in flavor (f) and color (c) space, whereas the charge conjugation operator C is already incorporated in the definition of the Nambu-Gorkov field Ψ . The effects of the current quark masses on the quark propagator are involved in the QCD superconductor. In perturbation theory, we have to first order in the current quark mass [9]

$$\Delta \mathbf{S}(q) \approx \begin{pmatrix} \frac{m}{2\mu} \frac{q_0 + q_{||}}{q_0^2 - \epsilon_q^2} & -\gamma^0 \left(\frac{m\mathbf{M}^\dagger \Lambda^+(\mathbf{q})}{2\mu} + \frac{\mathbf{M}^\dagger m \Lambda^-(\mathbf{q})}{2\mu} \right) \frac{G^*(q)}{q_0^2 - \epsilon_q^2} \\ -\gamma^0 \left(\frac{m\mathbf{M} \Lambda^-(\mathbf{q})}{2\mu} + \frac{\mathbf{M} m \Lambda^+(\mathbf{q})}{2\mu} \right) \frac{G(q)}{q_0^2 - \epsilon_q^2} & \frac{m}{2\mu} \frac{-q_0 + q_{||}}{q_0^2 - \epsilon_q^2} \end{pmatrix} \quad (2)$$

with $m = \text{diag}(m_u, m_d, m_d)$. Details on the derivation of this result including $\mathcal{O}(m^2)$ terms can be found in the Appendix-1 and Appendix-2 ^{#4}.

Using the color-identity (see Appendix-4)

$$\sum_a \frac{\lambda^{aT}}{2} \epsilon_c^A \frac{\lambda^a}{2} = -\frac{2}{3} \epsilon_c^A, \quad (3)$$

the gap function $G(q)$ in the CFL phase with massless quarks satisfies the following gap equation

$$G(p) = \frac{4g^2}{3} \int \frac{d^4 q}{(2\pi)^4} i\mathcal{D}(p - q) \frac{G(q)}{q_0^2 - \epsilon_q^2}$$

^{#2}Here $\bar{\psi}^T$ is the transposed and conjugated field and $C \equiv i\gamma^2\gamma^0$.

^{#3}Note that $\gamma^0\Lambda^\pm(\mathbf{q}) = \Lambda^\mp(\mathbf{q})\gamma^0$, $\gamma^5\Lambda^\pm(\mathbf{q}) = \Lambda^\pm(\mathbf{q})\gamma^5$ and $\boldsymbol{\alpha} \cdot \hat{\mathbf{q}}\Lambda^\pm(\mathbf{q}) = \pm\Lambda^\pm(\mathbf{q})$.

^{#4}In what follows, ‘‘Appendix- n ’’ denotes the item n in the Appendix.

$$= \frac{4g^2}{3} \int \frac{d^4 q_E}{(2\pi)^4} \mathcal{D}(p-q) \frac{G(q)}{q_4^2 + q_{||}^2 + |G(q)|^2} . \quad (4)$$

The second expression follows from Wick rotation to Euclidean space. For perturbative screening of gluons in the relevant ω, \vec{q} domain, the gluon-propagator in Euclidean space reads schematically as ^{#5}

$$\mathcal{D}(q) = \frac{1}{\frac{1}{2}q^2 + m_E^2} + \frac{1}{\frac{1}{2}q^2 + m_M^2} . \quad (5)$$

Perturbative arguments give $m_E^2/(g\mu)^2 = m_D^2/(g\mu)^2 \approx N_f/2\pi^2$ and $m_M^2/m_D^2 \approx \pi|q_4|/|4\mathbf{q}|$, where m_D is the Debye mass, m_M is the magnetic screening due to Landau damping and N_f the number of flavors [13]. To leading logarithm accuracy, the gap equation (4) can be solved using the logarithmic variables $x = \ln(\Lambda_*/p_{||})$, $y = \ln(\Lambda_*/q_{||})$, and $x_0 = \ln(\Lambda_*/G_0)$ [14], where $\Lambda_* = (4\Lambda_\perp^6/\pi m_E^5)$ and $\Lambda_\perp = 2\mu$. The result is

$$G(x) = G_0 \sin\left(\frac{\pi x}{2x_0}\right) = G_0 \sin\left(h_* x/\sqrt{3}\right) \quad (6)$$

with $h_* x_0/\sqrt{3} = \pi/2$ and G_0 given by

$$G_0 \approx \left(\frac{4\Lambda_\perp^6}{\pi m_E^5}\right) e^{-\frac{\sqrt{3}\pi}{2h_*}} , \quad (7)$$

where

$$h_*^2 \equiv \frac{g^2}{6\pi^2} . \quad (8)$$

This result is in agreement with [14, 15, 12], whereas in [11, 16, 17] there is an additional prefactor of 2. Note that $G(q)$ is a real-valued even function of $q_{||}$.

3. Generalized Scalar and Pseudoscalar Mesons

The generalized mesons will refer to excitations in qq as opposed to the standard mesons which are excitations in $\bar{q}q$ (see Appendix-9). The wavefunctions of the generalized scalar and pseudoscalar excitations in the QCD superconductor follows from the Bethe-Salpeter equation displayed in Fig. 1,

$$\mathbf{\Gamma}^A(p, P) = g^2 \int \frac{d^4 q}{(2\pi)^4} i\mathcal{D}(p-q) i\mathcal{V}_\mu^a i\mathbf{S}(q+\frac{P}{2}) \mathbf{\Gamma}^A(q, P) i\mathbf{S}(q-\frac{P}{2}) i\mathcal{V}_a^\mu , \quad (9)$$

where the gluon vertex is defined as a Nambu-Gorkov matrix (see Appendix-6)

$$\mathcal{V}_\mu^a \equiv \begin{pmatrix} \gamma_\mu \lambda^a/2 & 0 \\ 0 & C(\gamma_\mu \lambda^a/2)^T C^{-1} \end{pmatrix} = \begin{pmatrix} \gamma_\mu \lambda^a/2 & 0 \\ 0 & -\gamma_\mu \lambda^{aT}/2 \end{pmatrix} . \quad (10)$$

^{#5} This simplified version was used in [9, 12] and checked to be reliable for the leading logarithm results, see also Appendix-12.

The composite scalar vertex is given by

$$\mathbf{\Gamma}_\sigma^A(p, P) = \frac{1}{F_S} \begin{pmatrix} 0 & i\Gamma_S^*(p, P) (\mathbf{M}^A)^\dagger \\ i\Gamma_S(p, P) \mathbf{M}^A & 0 \end{pmatrix} \quad (11)$$

with $\mathbf{M}^A = \mathbf{M}^{i\alpha} (\tau^A)^{i\alpha}$ and $\mathbf{M}^{i\alpha} = \epsilon_f^i \epsilon_c^\alpha \gamma_5$. Note that $(\mathbf{M}^A)^\dagger = \epsilon_f^i \epsilon_c^\alpha \gamma_5 (\tau^{A*})^{i\alpha} = \epsilon_f^i \epsilon_c^\alpha \gamma_5 (\tau^A)^{\alpha i}$. The composite pseudoscalar vertex has been discussed in [9]. It reads

$$\mathbf{\Gamma}_\pi^A(p, P) = \frac{1}{F_{PS}} \begin{pmatrix} 0 & -i\gamma_5 \Gamma_{PS}^*(p, P) (\mathbf{M}^A)^\dagger \\ i\gamma_5 \Gamma_{PS}(p, P) \mathbf{M}^A & 0 \end{pmatrix}. \quad (12)$$

A thorough discussion of the spin-parity assignment for these vertices can be found in Appendix-7.

Inserting (1) in (9) we find, after a few reductions (see Appendix-8 for details), that both the scalar and pseudoscalar Bethe-Salpeter vertices obey

$$\Gamma(p, P) = \frac{4g^2}{3} \int \frac{d^4q}{(2\pi)^4} i\mathcal{D}(p-q) \frac{(Q_0 + Q_{||})(K_0 - K_{||}) - G(Q)G(K)}{(Q_0^2 - \epsilon_Q^2)(K_0^2 - \epsilon_K^2)} \Gamma(q, P) \quad (13)$$

with $Q = q + P/2$ and $K = q - P/2$ and $\Gamma(q, P) = \Gamma_S(q, P) = \Gamma_{PS}(q, P)$. In establishing (13) we have made use of the relations

$$\sum_a \frac{\lambda^{aT}}{2} (\mathbf{M}^A) \frac{\lambda^a}{2} = -\frac{2}{3} \mathbf{M}^A, \quad \sum_a \frac{\lambda^{aT}}{2} \left(\mathbf{M} (\mathbf{M}^A)^\dagger \mathbf{M} \right) \frac{\lambda^a}{2} \approx -\frac{2}{3} \mathbf{M}^A \quad (14)$$

(see Appendix-5) and ignored the symmetric contribution in color-flavor which is subleading in leading logarithm accuracy. In the meson rest frame $P = (M, \mathbf{0})$, we obtain

$$\Gamma(p, M) = \frac{4g^2}{3} \int \frac{d^4q}{(2\pi)^4} i\mathcal{D}(p-q) \frac{q_0^2 - \epsilon_q^2 - M^2/4}{(q_0^2 - \epsilon_q^2 + M^2/4)^2 - M^2 q_0^2} \Gamma(q, M). \quad (15)$$

This integral equation can be solved exactly in leading logarithm accuracy (see the analogous calculation in section 5). The resulting mass M in the present case is

$$M = 2G_0 \left(1 - e^{-(\sqrt{3}-\sqrt{3})\pi/h_*} \right)^{\frac{1}{2}} = 0, \quad (16)$$

which illustrates the Goldstone nature of the scalar and pseudoscalar excitations in the QCD superconductor. The pseudoscalar excitations are the generalized pions already discussed in [6, 9] with a form factor $\Gamma(q, 0) \propto G(q)$. The scalar excitations are would-be Goldstone modes that get eaten up by the longitudinal components of the colored gauge fields (see below).

Although (16) was derived using the simplified form (5), we now show that the outcome is the same, irrespective of that choice. Indeed, an alternative way of reaching the same result that is independent of the choice of the gluon propagator $\mathcal{D}(q)$ in (15), can

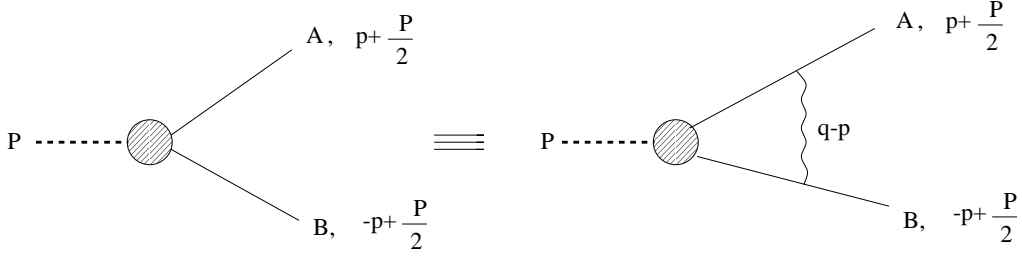


Figure 1: Bethe-Salpeter equation for the generalized mesons in the QCD superconductor.

be obtained by expanding the integrand in (15) in M^2 . For the Goldstone modes, this expansion is valid and we obtain (see Appendix-10)

$$iF^2 M^2 \approx \int \frac{d^4 q}{(2\pi)^4} \frac{\Gamma^2(q)}{q_0^2 - \epsilon_q^2} - \frac{3}{4g^2} \int d^4 x \frac{\Gamma^2(x)}{i\mathcal{D}(x)}, \quad (17)$$

where the second integration is over the configuration space (actually positive semidefinite in Euclidean space). Here M^2 is the Goldstone mass squared, and F ($= F_{PS} = F_S$) its decay constant with

$$F^2 \approx \frac{i}{4} \int \frac{d^4 q}{(2\pi)^4} \frac{q_0^2 + 3\epsilon_q^2}{(q_0^2 - \epsilon_q^2)^3} \Gamma^2(q). \quad (18)$$

Note that both M and F are functional of the form-factor $\Gamma(q)$. Minimizing the mass-functional with respect to $\Gamma(q)$ yields a gap-like equation with $\Gamma(q) = \kappa G(q)$ as a solution, modulo an arbitrary dimensionless constant κ . From (4) we observe in analogy to (17) that

$$\frac{3}{4g^2} \int d^4 x \frac{G^2(x)}{i\mathcal{D}(x)} = \int \frac{d^4 q}{(2\pi)^4} \frac{G^2(q)}{q_0^2 - \epsilon_q^2}. \quad (19)$$

Inserting (19) into (17) yields $F^2 M^2 \approx 0$, which implies massless Goldstone modes in the chiral limit, since F^2 is nonzero, i.e.

$$F^2 \approx \frac{\kappa^2 \mu^2}{8\pi^2} \int_0^\infty dq_{||} \frac{G^2(q_{||})}{\epsilon_q^3} = \frac{\kappa^2 \mu^2}{16\pi^2} \quad (20)$$

(see Appendix-10). For $\kappa = 4$ the result for F^2 is in agreement with the result established in [9], where the axial-vector current normalization has been used. The dependence of the mass of the generalized pion on the current quark mass can be estimated in mass perturbation theory using an axial-Ward identity [9], see the Appendix-3. The mass effects are of order m/μ , and to leading order, we have [9]

$$(M^2)^{\alpha\beta} = -\frac{\mu G_0}{4\pi^2 F_T^2} \text{Tr}_{cf} \left([m^2, \tau^\alpha] (\mathbf{M}^\dagger \mathbf{M}^\beta - \mathbf{M}^{\beta\dagger} \mathbf{M}) + [m^2, \tau^{\alpha*}] (\mathbf{M} \mathbf{M}^{\beta\dagger} - \mathbf{M}^\beta \mathbf{M}^\dagger) \right). \quad (21)$$

Using the weak coupling values for F_T and G_0 , (21) becomes

$$(M^2)^{\alpha\beta} = -\sqrt{\frac{2}{3}} \frac{256\pi^4}{9g^5} \exp\left(-\frac{3\pi^2}{\sqrt{2}g}\right) \left\{ \text{Tr}_{cf} \left([m^2, \tau^\alpha] (\mathbf{M}^\dagger \mathbf{M}^\beta - \mathbf{M}^{\beta\dagger} \mathbf{M}) \right) + \text{Tr}_{cf} \left([m^2, \tau^{\alpha*}] (\mathbf{M} \mathbf{M}^{\beta\dagger} - \mathbf{M}^\beta \mathbf{M}^\dagger) \right) \right\}. \quad (22)$$

The color-flavor traces in (21-22) yield zero. This is consistent with the fact that

$$\begin{aligned}\text{Tr}(m \rho_0 \mathbf{S}(q) m \rho_0 \mathbf{S}(q)) &= \text{Tr}(m S_{11}(q) m S_{11}(q)) + \text{Tr}(m S_{22}(q) m S_{22}(q)) \\ &= \frac{4}{\mu} \frac{q_{||}}{q_0^2 - \epsilon_q^2} \text{Tr}_{cf}(m^2) + \mathcal{O}(1/\mu^2),\end{aligned}\quad (23)$$

to second order in mass perturbation theory, where ρ_0 is the unit matrix in the Nambu-Gorkov space. Equation (23) follows after inserting the $S_{11}(q)$ and $S_{22}(q)$ Nambu-Gorkov components of the full massless propagator (A24), expanded to next-to-leading order in $1/\mu$, and is seen to vanish after the $q_{||}$ -integration is carried out. The vanishing of (23) to leading order in $1/\mu$ can be understood as follows: each mass insertion flips chirality but preserves helicity. Hence the quarks must carry opposite energies, which is not possible if the antiparticles are absent. Indeed, (23) vanishes to leading order because of the orthogonality of the massless energy projectors occurring in (1).

At next-to-leading order in $1/\mu$, however, the vanishing of the mass is averted by keeping the antiparticle content of $\mathbf{S}(q)$ as given in (A24) and using the simplified form (12) of the generalized-pion vertex. Note that the antiparticle gap, which according to [15] is gauge-fixing-term dependent (see also Appendix-12), does not appear at this order, but first at next-to-next-to-leading order (see Appendix-1 and Appendix-3). The mass of the Goldstone modes at next-to-leading order reads

$$\begin{aligned}(M^2)^{\alpha\beta} &\approx -\frac{G_0^2 x_0}{8\pi^2 F_T^2} \left\{ \text{Tr}_{cf}([m, \tau^\alpha]_+ (\mathbf{M}^{\beta\dagger} m \mathbf{M} + \mathbf{M}^\dagger m \mathbf{M}^\beta)) \right. \\ &\quad \left. + \text{Tr}_{cf}([m, \tau^{\alpha*}]_+ (\mathbf{M}^\beta m \mathbf{M}^\dagger + \mathbf{M} m \mathbf{M}^{\beta\dagger})) \right\} \\ &= -\frac{2^{18} \pi^{10}}{3^4 \sqrt{2} g^{11}} \exp\left(\frac{-3\sqrt{2} \pi^2}{g}\right) \left\{ \text{Tr}_{cf}([m, \tau^\alpha]_+ (\mathbf{M}^{\beta\dagger} m \mathbf{M} + \mathbf{M}^\dagger m \mathbf{M}^\beta)) \right. \\ &\quad \left. + \text{Tr}_{cf}([m, \tau^{\alpha*}]_+ (\mathbf{M}^\beta m \mathbf{M}^\dagger + \mathbf{M} m \mathbf{M}^{\beta\dagger})) \right\}\end{aligned}\quad (24)$$

in the general case $m_u \lesssim m_d \ll m_s$ and with the weak-coupling values for F_T , G_0 and x_0 (see Appendix-3). At next-to-leading order the pion mass relation (24) is reminiscent of the quadratic Gell-Mann-Oakes-Renner relation in the vacuum, as is explicit from the axial-Ward-identity [9]. Using the current mass decomposition

$$m \equiv \frac{1}{3} \text{Tr}(m) \mathbf{1} + m^\lambda \tau^\lambda = \hat{m} \mathbf{1} + m^\lambda \tau^\lambda, \quad (25)$$

$\mathbf{M} = \mathbf{M}^{aa} \equiv \epsilon_f^a \epsilon_c^a$ and $\mathbf{M}^\beta \equiv \mathbf{M}^{i\alpha} (\tau^\beta)^{i\alpha}$ ^{#6} and the identity

$$[\tau^\alpha, \tau^\beta]_+ = \frac{4}{3} \delta^{\alpha\beta} \mathbf{1} + 2d^{\alpha\beta\gamma} \tau^\gamma,$$

we can unwind the color-flavor traces in (24) to obtain the explicit mass matrix,

$$\begin{aligned}(M^2)^{\alpha\beta} &= \frac{2^{20} \pi^{10}}{3^4 \sqrt{2} g^{11}} \exp\left(\frac{-3\sqrt{2} \pi^2}{g}\right) \left\{ 8 \hat{m}^2 \delta^{\alpha\beta} + \frac{16}{3} m^\alpha m^\beta + 8 \hat{m} m^\lambda d^{\lambda\alpha\beta} \right. \\ &\quad \left. + 2 (\hat{m} m^\lambda \delta^{\alpha\sigma} + m^\lambda m^\gamma d^{\gamma\alpha\sigma}) \epsilon^{Inl} \epsilon^{Jsm} (\tau^\sigma)^{mn} (\tau^\beta + \tau^{*\beta})^{IJ} (\tau^\lambda)^{ls} \right\},\end{aligned}\quad (26)$$

^{#6}The γ_5 has been removed by the spin trace.

which is nonzero in the flavor symmetric case. Indeed, for $m_u = m_d = m_s \equiv m_q$, this result simplifies to

$$M^2 \approx \frac{2^{23} \pi^{10} m_q^2}{3^4 \sqrt{2} g^{11}} \exp\left(\frac{-3\sqrt{2} \pi^2}{g}\right), \quad (27)$$

showing the nonperturbative character of the Goldstone mass in the gauge coupling g . We have not checked whether the corrections to the leading logarithm approximation affects (26), since the leading order result (22) vanishes. An expression of similar structure to (27) can be found in [18].

At this stage, an important remark is in order: the non-vanishing of the next-to-leading order result depends on our simplification of the gluon-propagator (5), which leads to the subsequent simplification in the generalized meson vertices (11-12). Indeed, if we were to use the exact gluon-propagator (A78), then the generalized meson-vertices (11-12) (also (A61)) have to be changed to

$$\mathbf{\Gamma}_M^A(p, P) \longrightarrow \tilde{\mathbf{\Gamma}}_M^A(p, P) = \begin{pmatrix} \Lambda^-(\mathbf{p}) & 0 \\ 0 & \Lambda^+(\mathbf{p}) \end{pmatrix} \mathbf{\Gamma}_M^A(p, P) \begin{pmatrix} \Lambda^+(\mathbf{p}) & 0 \\ 0 & \Lambda^-(\mathbf{p}) \end{pmatrix}, \quad (28)$$

to satisfy the pertinent Bethe-Salpeter equations (see Appendix-12). The additional projectors in (28) cause the mass of the Goldstone modes to remain massless at next-to-leading order as well. We note that the additional projectors in (28) follow the structure of the leading quark propagator (1), and are in general superfluous if each vertex $\mathbf{\Gamma}_M^A$ is only linked by the *leading* part of the quark propagator. If the vertex is of a scalar or pseudoscalar nature, it is already sufficient that each vertex is coupled to at least *one leading* part of the quark propagator (see Appendix-7). This is the case of most our results to leading order, hence our simplification. The exception is (26) which is a next-to-leading order result, since two subleading propagators (a massive and a next-to-leading order massless one) are there attached to one vertex.

4. Higgs Mechanism

The generalized scalar mesons mix with the longitudinal gluons through the non-diagonal polarization

$$\Pi_\mu^{aA}(Q) = -ig \int \frac{d^4 q}{(2\pi)^4} \text{Tr} \left(i\mathcal{V}_\mu^a i\mathbf{S}(q + \frac{Q}{2}) i\mathbf{\Gamma}_\sigma^A(q, Q) i\mathbf{S}(q - \frac{Q}{2}) \right), \quad (29)$$

where $\mathbf{\Gamma}_\sigma^A(q, Q)$ is defined in (11). Since the scalar form factor is $\mathbf{\Gamma}_S(q, 0) = G(q)/F$, equation (29) can be reduced to

$$\Pi_\mu^{aA}(Q) = \frac{g}{F} \text{Tr} \left(\frac{\lambda^a}{2} \mathbf{M}^\dagger \mathbf{M}^A \right) \int \frac{d^4 q}{(2\pi)^4} \frac{G(q)}{(K_0^2 - \epsilon_K^2)(P_0^2 - \epsilon_P^2)}$$

$$\begin{aligned} & \times \left\{ \left[(K_0 + K_{||})G(P) - (P_0 + P_{||})G(K) \right] \text{Tr} [\gamma_0 \gamma_\mu \Lambda^+(K) \Lambda^+(P)] \right. \\ & \left. + \left[(K_0 - K_{||})G(P) - (P_0 - P_{||})G(K) \right] \text{Tr} [\gamma_0 \gamma_\mu \Lambda^-(K) \Lambda^-(P)] \right\} \end{aligned} \quad (30)$$

with $K = q + Q/2$ and $P = q - Q/2$. Clearly $\Pi_\mu(0) = 0$. In the following, we will use

$$\text{Tr} \left(\frac{\lambda^a}{2} \mathbf{M}^\dagger \mathbf{M}^A \right) \equiv \text{Tr}_f \text{Tr}_c \left(\frac{\lambda^a}{2} \mathbf{M}^\dagger \mathbf{M}^A \right) = -(\lambda^a)^{ji} (\tau^A)^{ji} = -\text{Tr} (\tau^a \tau^A) = -2\delta^{aA},$$

$\text{Tr}[\Lambda^+(K) \Lambda^+(P)] = \text{Tr}[\Lambda^-(K) \Lambda^-(P)] = 1 + \hat{\mathbf{K}} \cdot \hat{\mathbf{P}} \rightarrow 2$ and $\text{Tr}[\gamma_0 \gamma_i \Lambda^+(K) \Lambda^+(P)] = -\text{Tr}[\gamma_0 \gamma_i \Lambda^-(K) \Lambda^-(P)] = \hat{\mathbf{K}}^i + \hat{\mathbf{P}}^i \rightarrow 2\hat{\mathbf{q}}^i$ as well as $K_{||} - P_{||} \approx \hat{\mathbf{q}} \cdot \mathbf{Q}$. In this way, we obtain to linear order in Q ,

$$\begin{aligned} \Pi_0^{aA}(Q) & \approx i\delta^{aA} Q_0 g F_T, \\ \Pi_i^{aA}(Q) & \approx i\delta^{aA} Q_i g \frac{F_S^2}{F_T} = i\delta^{aA} Q_i g v^2 F_T. \end{aligned} \quad (31)$$

The temporal and spatial pion decay constants are, respectively [9]

$$F_T^2 \approx -8i \int \frac{d^4 q}{(2\pi)^4} \frac{G^2(q)}{(q_0^2 - \epsilon_q^2)^2}, \quad (32)$$

$$F_S^2 \approx -8i \int \frac{d^4 q}{(2\pi)^4} (\hat{\mathbf{q}} \cdot \hat{\mathbf{Q}})^2 \frac{G^2(q)}{(q_0^2 - \epsilon_q^2)^2}, \quad (33)$$

where $v^2 = F_S^2/F_T^2 = 1/3$ is the square of the velocity of the Goldstone modes [8, 9].

The nonvanishing of (31) implies that the 8 generalized scalars in the CFL phase are eaten up by the longitudinal gluons. As a result, the gluons acquire masses in a manner analogous to the familiar Meissner effect. Indeed, if we denote by Σ^{cf} the scalar color-flavor order parameter in the CFL phase, then under local color transformations $\Sigma \rightarrow g_c \Sigma$. In the local approximation (leading order in Q), the gluon-scalar mixing is described by the Higgs term

$$\mathcal{L}_H = \frac{1}{4} \text{Tr} |\partial_0 \Sigma - ig A_0 \Sigma|^2 - \frac{v^2}{4} \text{Tr} |\partial_i \Sigma - ig A_i \Sigma|^2. \quad (34)$$

For the scalar excitations, $\Sigma = F_T \lambda^0 + \sigma^A \lambda^A$ and (34) becomes

$$\begin{aligned} \mathcal{L}_H &= \frac{1}{2} \left(\dot{\sigma}^A \dot{\sigma}^A - v^2 \partial_i \sigma^A \partial_i \sigma^A \right) + \frac{g^2 F_T^2}{2} \left(A_0^A A_0^A - v^2 A_i^A A_i^A \right) \\ &\quad - g F_T \left(\dot{\sigma}^A A_0^A - v^2 \partial_i \sigma^A A_i^A \right). \end{aligned} \quad (35)$$

The mixing vertices in (35) are precisely the ones given by (31). If we define

$$\begin{aligned} \tilde{A}_0^A &= A_0^A - \frac{1}{g F_T} \partial_0 \sigma^A, \\ \tilde{A}_i^A &= A_i^A - \frac{1}{g F_T} \partial_i \sigma^A, \end{aligned} \quad (36)$$

then (35) reduces to

$$\mathcal{L}_H = \frac{g^2 F_T^2}{2} \tilde{A}_0^A \tilde{A}_0^A - \frac{g^2 F_S^2}{2} \tilde{A}_i^A \tilde{A}_i^A \quad (37)$$

which is purely a mass term for the new gluon field \tilde{A} . Originally there are 8 gluons A that are massless with two transverse polarizations. After the Higgs mechanism (36), the gluons become massive in the CFL phase, with the scalar making up the longitudinal component. No scalars are left. The Meissner mass (37) refers to the inverse penetration length of *static* colored magnetic fields in the QCD superconductor which is unexpectedly small, i.e. $1/g\mu$. In weak coupling the Meissner mass is of the order of the electric screening mass $m_E \approx g\mu$. It is not of the order of $g G_0$ as in a conventional superconductor with a constant (energy independent) gap. It is important to note that the *nonstatic gluonic modes* with $Q_0 > G_0$ sense ‘free quarks’ for which there is electric screening but no magnetic screening. A brief analysis of the polarization function in the CFL phase supporting this is given in the Appendix-11. The nonstatic and long-range magnetic effects are at the origin of the pairing mechanism discussed here, including the binding in the mesonic excitation spectrum.

5. Masses of Generalized Vector and Axial-Vector Mesons

In this section we consider vector mesons consisting of a pair of (quasi-)quarks or (quasi-)holes at the Fermi surface with momenta $p_1 = -q + P/2$ and $p_2 = q + P/2$. In the CFL phase these composites (generalized vector mesons) have finite size. Since Lorentz invariance is absent, there are electric and magnetic composite mesons. Their transverse and longitudinal vector form factors (or wavefunctions) $\Gamma_{T,L}^A$ in the Nambu-Gorkov representation are defined as

$$\Gamma_j^A(q, P) \equiv \gamma_j \Gamma_V^A(q, P) = \hat{\mathbf{P}}_j \hat{\mathbf{P}}^i \gamma_i \Gamma_L^A(q, P) + \left(-g_j^i - \hat{\mathbf{P}}_j \hat{\mathbf{P}}^i \right) \gamma_i \Gamma_T^A(q, P) \quad (38)$$

with

$$\Gamma_L^A = \int d\hat{\mathbf{P}} \gamma^k \hat{\mathbf{P}}_k \hat{\mathbf{P}}^j \Gamma_j^A, \quad (39)$$

$$\Gamma_T^A = \frac{1}{2} \int d\hat{\mathbf{P}} \gamma^k \left(g_k^j + \hat{\mathbf{P}}_k \hat{\mathbf{P}}^j \right) \Gamma_j^A. \quad (40)$$

Current conservation implies $P^\mu \Gamma_\mu^A(q, P) = 0$, such that the temporal form factor $\Gamma_0^A(p, P)$ is not an independent quantity, but can be expressed in terms of Γ_L^A as

$$\Gamma_0^A(p, P) = -\frac{\vec{\gamma} \cdot \vec{\mathbf{P}}}{P_0} \Gamma_L^A(p, P). \quad (41)$$

In the QCD superconductor this implies 1 electric (L) and 2 magnetic (T) modes for the composite vector mesons. The purpose of this section is to evaluate their form factors and “masses” (or more precisely excitation energies) in the weak coupling limit. For that, we note that the wavefunction (up to a dimensionful normalization) of the electric and magnetic

modes follow from the Bethe-Salpeter equation displayed in Fig. 1, i.e.

$$\mathbf{\Gamma}_\nu^A(p, P) = g^2 \int \frac{d^4 q}{(2\pi)^4} i\mathcal{D}(p - q) i\mathcal{V}_\mu^a i\mathbf{S}(q + \frac{P}{2}) \mathbf{\Gamma}_\nu^A(q, P) i\mathbf{S}(q - \frac{P}{2}) i\mathcal{V}_a^\mu, \quad (42)$$

where the gluon vertex is defined in (10). As discussed in the Appendix-7, the composite vector meson vertices for the transverse and longitudinal modes have the following structure

$$\mathbf{\Gamma}_{T,L}^A(p, P) = \frac{1}{F_V} \begin{pmatrix} 0 & \mathbf{\Gamma}_{T,L}^*(p, P) (\mathbf{M}^A)^\dagger \\ \mathbf{\Gamma}_{T,L}(p, P) \mathbf{M}^A & 0 \end{pmatrix}. \quad (43)$$

Inserting (1) in (42) we find, after a few reductions (see the Appendix-8 for details),

$$\Gamma_{T,L}(p, P) = \frac{4g^2}{9} \int \frac{d^4 q}{(2\pi)^4} i\mathcal{D}(p - q) \frac{(Q_0 + Q_\parallel)(K_0 - K_\parallel) - G(Q)G(K)}{(Q_0^2 - \epsilon_Q^2)(K_0^2 - \epsilon_K^2)} \Gamma_{T,L}(q, P) \quad (44)$$

with $Q = q + P/2$ and $K = q - P/2$.

In the rest frame of the composite vector meson, $P = (M_V, \mathbf{0})$, equation (44) becomes

$$\Gamma_{T,L}(p, M_V) = \frac{4g^2}{9} \int \frac{d^4 q}{(2\pi)^4} i\mathcal{D}(p - q) \frac{q_0^2 - \epsilon_q^2 - M_V^2/4}{(q_0^2 - \epsilon_q^2 + M_V^2/4)^2 - M_V^2 q_0^2} \Gamma_{T,L}(q, M_V), \quad (45)$$

where we have used that $\Gamma_{T,L}(q, M_V)$ is an even real function of q . The difference between the vector equation (45) and the scalar equation (15) is in the prefactors : 4/9 versus 4/3 respectively. As a result, (15) admits massless modes, while (45) does not. Indeed, using (5) in (45) and assuming that $\Gamma_{T,L}(q, M_V) \approx \Gamma_{T,L}(q_\parallel, M_V)$ with support only around the Fermi surface, we get, after a few integrations ^{#7}

$$\begin{aligned} \Gamma_{T,L}(p_\parallel, M) &\approx \frac{h_*^2}{36} \int_0^\infty dq_\parallel \left(\frac{1}{\sqrt{q_\parallel^2 + |G(q_\parallel)|^2} - M_V/2} + \frac{1}{\sqrt{q_\parallel^2 + |G(q_\parallel)|^2} + M_V/2} \right) \\ &\times \ln \left\{ \left(1 + \frac{\Lambda_\perp^2}{(p_\parallel - q_\parallel)^2 + m_E^2} \right)^3 \left(1 + \frac{\Lambda_\perp^3}{|p_\parallel - q_\parallel|^3 + \frac{\pi}{4} m_D^2 |p_\parallel - q_\parallel|} \right)^2 \right\} \\ &\times \Gamma_{T,L}(q_\parallel, M). \end{aligned} \quad (46)$$

Since $|p_\parallel - q_\parallel| \ll m_E = m_D \ll \Lambda_\perp = 2\mu$, equation (46) is simplified in leading logarithm accuracy to

$$\Gamma_{T,L}(p_\parallel, M_V) \approx \frac{h_*^2}{18} \int_{G_M}^{\Lambda_*} \frac{dq_\parallel}{q_\parallel} \ln \left(\frac{\Lambda_*^2}{(p_\parallel - q_\parallel)^2} \right) \Gamma_{T,L}(q_\parallel, M_V) \quad (47)$$

^{#7}The logarithms result from the q_\perp integration. The contour integration in q_0 is performed under the assumption that $\mathcal{D}(p - q)$ is dominated by nearly static contributions, where the following identity is used:

$$\frac{q_0^2 - \epsilon_q^2 - M_V^2/4}{(q_0^2 - \epsilon_q^2 + M_V^2/4)^2 - M_V^2 q_0^2} = \frac{1}{2} \left(\frac{1}{q_0^2 - (\epsilon_q - M_V/2)^2} + \frac{1}{q_0^2 - (\epsilon_q + M_V/2)^2} \right).$$

The remaining steps are analogous to the ones discussed in [12]. The coefficient h_* is defined in (8).

with

$$G_M^2 = G_0^2 - M_V^2/4 \quad (48)$$

and $\Lambda_* = 4\Lambda_\perp^6/\pi m_E^5$. The solution to (47) is obtained by using the new logarithmic variables $x = \ln(\Lambda_*/p_\parallel)$ and $x_M = \ln(\Lambda_*/G_M)$ as discussed in [12]. Following this reference, the transverse and longitudinal form factors for the composite vector mesons are found to be equal to

$$\Gamma_{T,L}(p_\parallel, M_V) \approx G_M \sin\left(\frac{\pi x}{2x_M}\right) = \sqrt{G_0^2 - \frac{M_V^2}{4}} \sin\left(\frac{h_*}{3} \ln\left(\frac{\Lambda_*}{p_\parallel}\right)\right) \quad (49)$$

with

$$\frac{h_*}{3} \ln\left(\frac{\Lambda_*}{G_M}\right) = \frac{h_*}{3} x_M = \frac{\pi}{2} . \quad (50)$$

Notice the threshold singularity for pair production at $M_V = 2G_0$. Using (48), (50) and (7), we get the following value for the mass M_V of the generalized vector meson

$$M_V = 2G_0 \left(1 - e^{-(3-\sqrt{3})\pi/h_*}\right)^{\frac{1}{2}} . \quad (51)$$

We recall that $h_* = g/(\sqrt{6}\pi)$. Note that M_V is less than $2G_0$. Thus the composite pairs of particles or holes are bound exponentially weakly in the CFL phase. The smaller the coupling, the smaller the binding. For $g \rightarrow 0$, we reach the breaking of the composite pair, and their mass asymptotes $2G_0$. For g large their mass asymptotes zero which we interpret as a realization of Georgi's vector limit [19] in dense QCD. A rerun of these arguments for the axial-vector composites yield the same mass (see Appendix-8). In the CFL superconductor both the vector and axial-vector octets are degenerate in leading logarithm approximation, in spite of chiral symmetry breaking.

6. Vector Meson Coupling to Currents

The dimensionful coupling F_V of the vector mesons in the QCD superconductor is defined by

$$\langle \text{BCS} | \mathbf{V}_\mu^\alpha(0) | V_{T,L}^A(P) \rangle \equiv F_V M_V \mathcal{E}_\mu^{T,L}(P) \delta^{\alpha A} , \quad (52)$$

where $\langle \text{BCS} |$ stands for the CFL ground state and $\mathcal{E}_\mu^{T,L}$ are the transverse and longitudinal polarizations. In terms of the original quark fields Ψ , the vector current follows from Noether theorem. Hence (see Appendix-6)

$$\mathbf{V}_\mu^\alpha(x) = \bar{\Psi} \gamma_\mu \frac{1}{2} \mathbf{T}^\alpha \rho_3 \Psi \quad (53)$$

with $\mathbf{T}^A = \text{diag}(\tau^A, \tau^{A*})$ an $SU(3)_{c+F}$ valued generator in the Nambu-Gorkov representation and ρ_3 the standard Pauli matrix acting on the Nambu-Gorkov indices, in accordance

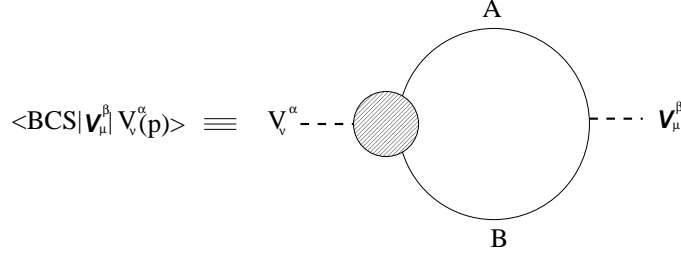


Figure 2: Vector transition in the QCD superconductor.

with (10). A diagrammatic representation of (52) is shown in Fig. 2. Inserting (53) in (52), we obtain from Fig. 2

$$F_V M_V \mathcal{E}_\mu^{T,L}(P) \delta^{\alpha A} = - \int \frac{d^4 k}{(2\pi)^4} \text{Tr} \left(\gamma_\mu \frac{1}{2} \mathbf{T}^\alpha \boldsymbol{\rho}_3 i\mathbf{S}(k + \frac{P}{2}) i\mathcal{E}_\nu^{T,L}(P) \mathbf{\Gamma}_V^{\nu A}(k, P) i\mathbf{S}(k - \frac{P}{2}) \right) \quad (54)$$

with $\mathbf{\Gamma}_V^{\nu A}$ as defined in (38). However, because of the spin structure,

$$\text{Tr}_s(\gamma_\mu \gamma_0 \gamma_r \alpha^n) = 0, \quad n = 0, 1, 2, \dots, \quad (55)$$

the right hand side of (54) vanishes identically, to leading logarithm accuracy and in the chiral limit.

So, the vector excitations couple to the usual physical currents only in subleading order if at all. An exact and direct assessment of this coupling is beyond the scope of the present work. Instead, we will present a variational estimate for F_V (temporal) based on the variational analysis discussed in section 3 for the scalars and pseudoscalars (massless excitations) which turn out to compare well with the exact results. Indeed, a rerun of the variational arguments, i.e. the application of the steps between (15) and (17) to (45), yields

$$\begin{aligned} F_V^2 &\approx \frac{\mu^2}{8\pi^2} \int_0^\infty dq_{||} \frac{\Gamma_{T,L}^2(q_{||}, M_V)}{\epsilon_q^3} \approx \frac{\mu^2}{8\pi^2} \int_{G_0}^{\Lambda_*} dq_{||} \frac{\kappa^2 G_M^2 \sin^2\left(\frac{h_*}{3} \ln\left(\frac{\Lambda_*}{q_{||}}\right)\right)}{q_{||}^3} \\ &= \frac{\kappa^2 \mu^2}{8\pi^2} \frac{G_M^2}{G_0^2} \int_0^{x_0} dx e^{2(x-x_0)} \sin^2\left(\frac{\pi x}{2x_M}\right) = \frac{\kappa^2 \mu^2}{8\pi^2} \frac{G_M^2}{G_0^2} \frac{1 - \cos(\pi x_0/x_M)}{4} \\ &= \frac{\kappa^2 \mu^2 (1 - \cos(\pi/\sqrt{3}))}{32\pi^2} e^{-\frac{\pi}{h_*}(3-\sqrt{3})}. \end{aligned} \quad (56)$$

The ratio $F_V^2/F^2 \ll 1$ is indeed subleading in weak coupling. Similar variational arguments for the vector mass yields an upper bound of the form (see Appendix-10)

$$M_V^2 \leq 8x_0 G_0^2 \frac{2(1 - (x_M/\pi x_0) \sin(\pi x_0/x_M))}{1 - \cos(\pi x_0/x_M)}, \quad (57)$$

which is generously satisfied by the exact result (51).

The generalized vector meson coupling to the scalars can be assessed similarly, by substituting in Fig. 2 the vector current by the generalized scalar vertex, i.e.

$$\mathbf{\Pi}_i^{aA}(P) = -i \int \frac{d^4 k}{(2\pi)^4} \text{Tr} \left(i\mathbf{\Gamma}_i^a(k, P) i\mathbf{S}(k + \frac{P}{2}) i\mathbf{\Gamma}_\sigma^A(k, P) i\mathbf{S}(k - \frac{P}{2}) \right). \quad (58)$$

Substituting for the vector and scalar vertex, we obtain

$$\begin{aligned} \Pi_i^{aA}(P) &= \frac{1}{F_V F_S} \text{Tr} \left(\mathbf{M}^a \mathbf{M}^{A\dagger} \right) \int \frac{d^4 k}{(2\pi)^4} \frac{(Q_0 - Q_{||})(K_0 + K_{||}) - (Q_0 + Q_{||})(K_0 - K_{||})}{(Q_0^2 - \epsilon_Q^2)(K_0^2 - \epsilon_K^2)} \\ &\quad \times \Gamma_V(k, P) \Gamma_S(k, P) \text{Tr} (\gamma_i \Lambda^+(\mathbf{Q}) \Lambda^+(\mathbf{K})) \end{aligned} \quad (59)$$

with $Q = k + P/2$ and $K = k - P/2$. The spin trace in (59) is found to vanish. In leading logarithm approximation, the generalized vectors and scalars do not mix, in contrast to the mixing between the generalized scalars and gluons which is at the origin of the Higgs mechanism discussed in section 4. Mixing may take place at next-to-leading order with consequences on leptonic emissivities in dense matter.

7. Vector Meson Coupling to Goldstones

The composite character of the vector mesons in the CFL phase allows them to interact with the generalized pions in the QCD superconductor modulo G-parity. Indeed, the decay process $V \rightarrow \pi$ (and in general any odd number of π) can be easily seen to vanish in the CFL phase. In this section, we will estimate the $V \rightarrow \pi\pi$ decay in the CFL phase as represented by Fig. 3 in leading logarithm accuracy and in the chiral limit.

The effective vertex associated to Fig 3, translates to the following equation

$$\begin{aligned} \mathcal{V}_\mu^{ABC}(P, Q) &= - \int \frac{d^4 q}{(2\pi)^4} \text{Tr} \left(i\mathbf{S}(q + \frac{P}{2}) i\gamma_\mu \mathbf{\Gamma}_V^A(q, P) i\mathbf{S}(q - \frac{P}{2}) i\mathbf{\Gamma}_\pi^B(q - \frac{Q}{2}, P - Q) \right. \\ &\quad \left. \times i\mathbf{S}(q - Q + \frac{P}{2}) i\mathbf{\Gamma}_\pi^C(q + \frac{P - Q}{2}, Q) \right). \end{aligned} \quad (60)$$

The composite vector and composite pion vertices are given, respectively, by (43) inserted into (38) and by (12). The general structure of the vertex (38) and the lack of Lorentz invariance in the CFL phase yield eight form factors,

$$\begin{aligned} \mathcal{V}_\mu^{ABC}(P, Q) &= +f^{ABC} \left\{ h_E^f(P, Q) P_0 + g_E^f(P, Q) Q_0 \right\} \delta_{\mu 0} \\ &\quad +f^{ABC} \left\{ h_M^f(P, Q) \mathbf{P}_i + g_M^f(P, Q) \mathbf{Q}_i \right\} \delta_{\mu i} \\ &\quad +d^{ABC} \left\{ h_E^d(P, Q) P_0 + g_E^d(P, Q) Q_0 \right\} \delta_{\mu 0} \\ &\quad +d^{ABC} \left\{ h_M^d(P, Q) \mathbf{P}_i + g_M^d(P, Q) \mathbf{Q}_i \right\} \delta_{\mu i}. \end{aligned} \quad (61)$$

The electric and magnetic couplings are $g_E \approx g_E(0, 0)$ and $g_M \approx g_M(0, 0)$. Setting $P = 0$ and $Q = (M, 0)$, the electric coupling is seen to vanish because of the mismatch in spin structure (i.e., tracing to an uncompensated γ_0 , see (55)) in the chiral limit, i.e. $g_E = 0$. Setting $P = 0$ and $Q = (0, \mathbf{Q})$ fixes the magnetic coupling. In terms of (43) the composite

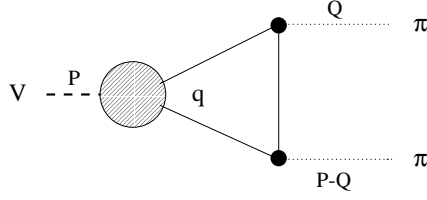


Figure 3: $V \rightarrow \pi\pi$ decay in the QCD superconductor.

vertex reads

$$\begin{aligned}
\mathcal{V}_{T,L}^{ABC}(P, Q) = & \frac{1}{F_V F^2} \int \frac{d^4 q}{(2\pi)^4} \Gamma_{T,L}(q, M_V) G^2(q - \frac{Q}{2}) \frac{1}{(q_0^2 - \epsilon_q^2)^2} \frac{1}{q_0^2 - \epsilon_{q-Q}^2} \\
& \times \text{Tr}_{fc} \left(\tau^A [\tau^B, \tau^C]_+ \right) \\
& \times \{ G(q) [q_- Q_+ - q_+ Q_-] \\
& \quad \times \text{Tr}_s [\Lambda^-(\mathbf{q}) \gamma_{T,L} \Lambda^-(\mathbf{q}) \Lambda^-(\mathbf{q} - \mathbf{Q}) + (\Lambda^- \rightarrow \Lambda^+)] \\
& \quad - G(q - Q) [q_+ q_- - 2G(q)^2] \\
& \quad \times \text{Tr}_s [\Lambda^-(\mathbf{q}) \gamma_{T,L} \Lambda^-(\mathbf{q}) \Lambda^-(\mathbf{q} - \mathbf{Q}) - (\Lambda^- \rightarrow \Lambda^+)] \}
\end{aligned} \tag{62}$$

with $q_{\pm} = q_0 \pm q_{||}$, $Q_{\pm} = \pm Q_{||}$ and $\gamma_{L,T} = \gamma_i \mathcal{E}_i^{LT}$. Equation (62) is identically zero, since the spin structure is of the form

$$\text{Tr}_s(\gamma^{\mu} \alpha^n) = 0 \quad \text{for } \mu = 0, 1, 2, 3 \quad \text{and } n = 0, 1, 2, \dots$$

In fact, one could have seen this already by inspecting (60) as it contains only one γ^{μ} and always an even number of γ^0 's (either 2 or 0) from the propagator (1) (either one S_{11} and one S_{22} appear together or only S_{12} 's and S_{21} 's). This holds for any value of P and Q . Hence $V \rightarrow \pi\pi$ vanishes to leading logarithm accuracy and in the chiral limit in the CFL phase, making the vector excitations real (zero width).

8. Vector Meson Mixing with Gluons

In the CFL phase the static electric and magnetic gluons are respectively screened and expelled (Meissner effect). Both the screening mass and the Meissner mass are of order $g\mu$ which is large on the scale of the superconductor excitations. So for all purposes, the static gluons decouple. For the *nearly static* gluons with energy $Q_0 \approx G_0$, both the screening and the Meissner effect in the superconductor weakens substantially. Indeed, it is the *nearly static magnetic gluons* which are not screened but only Landau damped that cause the

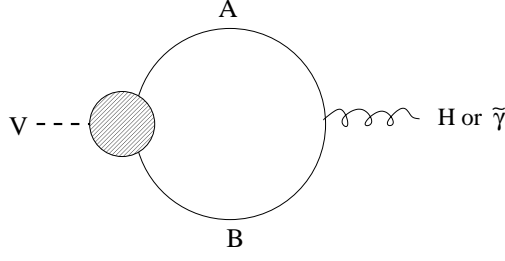


Figure 4: Composite vector meson transition into a gluon (H) or a tilde photon ($\tilde{\gamma}$) in the QCD superconductor.

binding of the composite pairs and their excitations in weak coupling with a magnetic scale m_M . In weak coupling, the vector mesons are dominant with $M_V \ll m_M$.

To analyze the mixing of the transverse composite vector mesons with the transverse magnetic gluons in the intermediate regime $M_V \sim m_M$, we define the 2-component vector fields (ρ_i^A, H_i^A) . Then the mixed propagator for the transverse modes reads

$$\begin{pmatrix} \Delta_V^{-1}(Q) & \Pi(Q) \\ \Pi(Q) & \Delta_H^{-1}(Q) \end{pmatrix}_{ij}^{\alpha\beta}, \quad (63)$$

where the diagonal transverse propagators are

$$\begin{aligned} \Delta_{V,ij}^{-1,\alpha\beta}(Q) &= \delta^{\alpha\beta} \left(\delta_{ij} - \hat{\mathbf{Q}}_i \hat{\mathbf{Q}}_j \right) (Q_0^2 - v_V^2 \mathbf{Q}^2 - M_V^2)^{-1} F_{V,T}^2, \\ \Delta_{H,ij}^{-1,\alpha\beta}(Q) &= \delta^{\alpha\beta} \left(\delta_{ij} - \hat{\mathbf{Q}}_i \hat{\mathbf{Q}}_j \right) (Q_0^2 - v_H^2 \mathbf{Q}^2 - M_H^2)^{-1} F_{H,T}^2 \end{aligned} \quad (64)$$

with $v^2 = F_S^2/F_T^2$. For the magnetic gluons $F_{H,T}$ and $F_{H,S}$ are related to the electric color susceptibility and magnetic permittivity in the superconductor. Their explicit form will not be needed for our arguments. The off-diagonal part of the mixed propagator (63) follows from Fig. 4. Hence

$$\Pi_{ij}^{\alpha\beta}(Q) = -ig \int \frac{d^4 q}{(2\pi)^4} \text{Tr} \left(\mathcal{V}_i^\alpha i\mathbf{S}(q + \frac{Q}{2}) i\mathbf{\Gamma}_j^\beta(q, Q) i\mathbf{S}(q - \frac{Q}{2}) \right) \quad (65)$$

which is found to vanish because one of the γ_0 from \mathbf{S} is not compensated at the gluon edge, see also (55). In the chiral limit and in leading logarithm accuracy, therefore, the composite and transverse vector mesons decouple from the transverse gluons. If any, mixing must occur at next-to-leading logarithm order or under explicit breaking of chiral symmetry.

9. Hidden Gauge Symmetry

We have seen that in weak coupling, the composite vector mesons are distinct from the screened and Higgsed gluons. Could they be the realization of a hidden local symmetry

in the CFL phase, besides the explicit local color symmetry? Furthermore, could the hidden local symmetry of the flavor sector be “dual” to the local color symmetry?^{#8} To answer these particular questions, we recall that in the CFL phase the color-flavor locking generates multidegenerate phases [21, 22], characterized by the following order parameter

$$\left\langle \overline{\Psi}(x) \mathbf{M}^{i\alpha} \left(e^{-i\gamma_5 \pi^A \mathbf{T}^A} \right)^{i\alpha} \rho_2 \Psi(y) \right\rangle \neq 0. \quad (66)$$

Recall $\mathbf{M}^{i\alpha} = \epsilon_f^i \epsilon_c^\alpha \gamma_5$, ρ_2 a Pauli matrix active on the Nambu-Gorkov entries, and $\mathbf{T}^A = \text{diag}(\tau^A, \tau^{A,*})$ an $SU(3)_{c+F}$ valued generator in the Nambu-Gorkov representation. The CFL phase is invariant under the diagonal of rigid vector-color plus vector-flavor, i.e. $SU(3)_{c+V}$.

As suggested in [9], in the CFL phase the generalized pions can be regarded as bound states of pairs of particles or holes. Because of the degeneracy (66), they may also be approximately described by $SU(3)_{c+A}$ valued excitations in the coset $(SU(3)_c \times SU(3)_L \times SU(3)_R)/SU(3)_{c+V}$, in the long-wavelength and zero-size limit [6, 7]. We note that (66) can also be rewritten as

$$\left\langle \overline{\Psi}(x) \mathbf{M}^{i\alpha} \left(\xi_f^{-1} \xi_c^{-1} \right)^{i\alpha} \rho_2 \Psi(y) \right\rangle = \left\langle \overline{\Psi}(x) \left(\xi_f^T \epsilon_f^\alpha \xi_f \right) \left(\xi_c^T \epsilon_c^\alpha \xi_c \right) \gamma_5 \rho_2 \Psi(y) \right\rangle \neq 0, \quad (67)$$

where we have used the unitary gauge $\xi_c = \xi_f = e^{i\gamma_5 \pi^A \mathbf{T}^A/2}$, and the identity

$$(\epsilon^c)^{\alpha\beta} \left(\xi^{-1} \right)^{cc'} \equiv \epsilon^{c\alpha\beta} \left(\xi^{-1} \right)^{cc'} = \left(\xi^T \epsilon^{c'} \xi \right)^{\alpha\beta}. \quad (68)$$

For constant π^A , the rigid rotations ξ_f and ξ_c can be reabsorbed through $\xi_f \xi_c \Psi \rightarrow \Psi$, leaving invariant the equations in the QCD superconductor. This rigid degeneracy is at the origin of the Goldstone modes in the CFL phase.

For composite pairs we observe that (67) enjoys a local symmetry through

$$e^{i\gamma_5 \pi^A \mathbf{T}^A} = \xi_f \xi_c = \xi_f h(x)^{-1} h(x) \xi_c, \quad (69)$$

where $h(x)$ is an element of local $SU(3)_{c+V}$. For *finite size* pairs, the local invariance (69) cannot be transported and reabsorbed in the fermionic fields $\Psi(x)$ and $\Psi(y)$ as they carry different arguments. Hence, strictly speaking, there is no hidden symmetry for local $SU(3)_{c+V}$ besides the original local color symmetry, in general.

However, in the limiting case where $x \rightarrow y$, and the size of the pair can be ignored^{#9}, then (69) is a hidden symmetry in the QCD superconductor. Indeed, the effective phases

^{#8} A similar issue is addressed in [20] in a different context.

^{#9} We stress that our exact calculation was rendered possible by the natural cutoff provided by the finite size of the composite. To what extent the zero-size approximation can be valid is not clear for the system in question. This caveat may seem to also apply to effective field descriptions of hadrons in zero-density environment. The light-quark hadrons such as π , ρ , ω etc. in the matter-free vacuum are of course finite-sized but nonetheless can be given an effective field theory description in terms of local chiral Lagrangians with hidden gauge symmetry etc. In such a description, the finite size is naturally accounted for by higher-order terms in chiral perturbation series. The resolution of this issue in the present case will have to involve going beyond the weak coupling and leading-log approximations that are not addressed here.

$\xi_{f,c}$ can be made local, and their corresponding effective action is invariant under the transformations [6]

$$\xi_f(x) \rightarrow g_f \xi_f(x) h^{-1}(x), \quad \xi_c(x) \rightarrow h(x) \xi_c(x) g_c^{-1}, \quad (70)$$

where g_f and g_c are rigid flavor and color transformations. The effective action for $\xi_f(x)$ and $\xi_c(x)$ or equivalently their chiral left-right unitary fields, in the zero size approximation was originally discussed in [6]. As a result of the local invariance (70), the vector mesons composed of pairs of particles or holes can be regarded as gauge particles of the hidden and local $SU(3)_{c+V}$ in the zero size approximation ^{#10}. They couple minimally to the generalized pions, and their properties follow from general principles [23]. In particular, their mass is given as $M_V^2 = 2F^2 g_{V\pi\pi}^2$ (KS RF-II) and their coupling to the CFL photon is $g_V = 2F^2 g_{V\pi\pi}$ (KS RF-I), which are both seen to mix orders in weak coupling. In the normal (non-superconducting) phase, the photons only couple through ρ -mesons leading to the concept of vector dominance (VDM), which is usually manifest through $g_{V\pi\pi} = g_{SU(3)_{c+V}}$ (universality). In this limit, the hidden gauge symmetry must be identical to the broken color symmetry $SU(3)_c$.

Since the pairs in the QCD superconductor have finite size, our results show that the concepts of hidden gauge symmetry and VDM are only approximate ^{#11}, and do not hold in weak coupling and leading-log approximation. We recall that in weak coupling, the pairs are very close in space (separation of order $1/\mu$) but far in time (separation of order $1/m_M \approx 1/(m_E^2 G_0)^{1/3} \gg 1/\mu$).

10. Conclusions

We have analyzed the generalized scalar, pseudoscalar, vector and axial-vector excitations in the CFL superconductor in the weak coupling limit. We have confirmed that the octet scalar and pseudoscalar excitations are both massless, and that only the pseudoscalars survive as Goldstone modes, while the scalars are Higgsed by the gluons leading to the Meissner effect. We have found that the vectors and axial vectors are bound and degenerate irrespective of their polarization, with a mass that is less than $2G_0$. Chiral symmetry is explicitly realized in the vector spectrum in the CFL phase in leading logarithm

^{#10}In [7], the hidden gauge symmetry was identified with the local color gauge group. Here it is clearly a local symmetry of the QCD superconductor when the pairs are assumed of zero size. The corresponding gauge particles are composite pairs of particles and holes as noted in [6]. The hidden gauge symmetry arrived at zero-size limit may be implying a “dual” relation between the two as in [20].

^{#11}It is not surprising that such concepts make precise sense only for modes that can be described by local fields. This situation is analogous to the role of VDM in baryon structure. Because of the finite skyrmion size, large N_c effective theories implemented with VDM are not as successful for baryon electromagnetic properties as they are for mesons.

approximation, in spite of its breaking in general. In the CFL superconductor the vector mesons are characterized by form factors that are similar but not identical to those of the generalized pions.

We have explicitly shown that the composite vector mesons can be viewed as a gauge manifestation of a hidden local $SU(3)_{c+V}$ when their size is ignored (their form factor set to one). In this limit, the effective Lagrangian description suggested in [6, 7, 8] is valid with the vector mesons described as Higgsed gauge bosons. Only in this limit, which is clearly approximative, do we recover concepts such as vector dominance and universality. (This is of course what one would expect in the QCD vacuum as well.) In any event, the zero-size limit is not compatible with the weak-coupling limit, because of the long-range pairing mechanism at work at large quark chemical potential. It is an open question whether going beyond the weak-coupling and leading-log approximations would render the concepts of effective field theories (e.g., HGS, VDM etc.) more appropriate.

Although our arguments were exclusive to the CFL phase, it is clear that they can be minimally changed to accommodate for the case of $N_f = 2$, which shows a qualitatively different form of superconductivity without color-flavor locking, in particular there are no generalized pions. Modulo some color-flavor factors, we have checked that our results carry over to the vector and axial-vector excitations. They change minimally for the scalars at the origin of the Higgs mechanism, also present for two flavors.

The existence of bound light scalar, vector and axial-vector mesons in QCD at high density, may have interesting consequences on dilepton and neutrino emissivities in dense environments such as the ones encountered in neutron stars. For example, in young and hot neutron stars neutrino production via quarks in the superconducting phase can be substantially modified if the vector excitations are deeply bound with a non-vanishing coupling, a plausible situation in QCD in strong coupling. These excitations may be directly seen by scattering electrons off compressed nuclear matter (with densities that allow for a superconducting phase to form) and may cause substantial soft dilepton emission in the same energy range in “cold” heavy-ion collisions.

Acknowledgments

We thank Youngman Kim for help with the figures. MR thanks Deog Ki Hong, Hyun Kyu Lee and Maciek Nowak for discussions. This work was supported in part by US-DOE DE-FG-88ER40388 and DE-FG02-86ER40251.

Appendix

In this appendix, we give some of the missing steps in deriving the formulae of the main text.

1. Direct calculation of the propagator (1) including mass corrections (2):

According to Ref. [10], the general entries for $\mathbf{S}(q)$ read

$$\begin{aligned} S_{11}(q) &= -i \langle \psi(q) \bar{\psi}(q) \rangle = \left\{ \left(G_0^+(q) \right)^{-1} - \gamma^0 \Delta^\dagger(q) \gamma^0 G_0^-(q) \Delta(q) \right\}^{-1}, \\ S_{12}(q) &= -i \langle \psi(q) \bar{\psi}_C(q) \rangle = -G_0^+(q) \gamma^0 \Delta^\dagger(q) \gamma^0 S_{22}(q), \\ S_{21}(q) &= -i \langle \psi_C(q) \bar{\psi}(q) \rangle = -G_0^-(q) \Delta(q) S_{11}(q), \\ S_{22}(q) &= -i \langle \psi_C(q) \bar{\psi}_C(q) \rangle = \left\{ \left(G_0^-(q) \right)^{-1} - \Delta(q) G_0^+(q) \gamma^0 \Delta^\dagger(q) \gamma^0 \right\}^{-1} \end{aligned} \quad (\text{A1})$$

with

$$\begin{aligned} \left(G_0^\pm(q) \right)^{-1} &= \gamma_\mu q^\mu \pm \mu \gamma^0 - m \\ &= \gamma^0 (q_0 \pm \mu - \boldsymbol{\alpha} \cdot \mathbf{q}) - m, \end{aligned} \quad (\text{A2})$$

where, in general $m = \text{diag}(m_u, m_d, m_s)$. Furthermore,

$$\Delta(q) = \mathbf{M} G(q) \Lambda^+(\mathbf{q}) + \mathbf{M} \bar{G}(q) \Lambda^-(\mathbf{q}), \quad (\text{A3})$$

where $\mathbf{M} = \epsilon_f^a \epsilon_c^a \gamma_5 = \mathbf{M}^\dagger$ with $(\epsilon^a)^{bc} = \epsilon^{abc}$. Note that

$$\gamma^0 \Delta^\dagger(q) \gamma^0 = -\mathbf{M}^\dagger G^*(q) \Lambda^-(\mathbf{q}) - \mathbf{M}^\dagger \bar{G}^*(q) \Lambda^+(\mathbf{q}) \quad (\text{A4})$$

and

$$\left(\mathbf{M}^\dagger \mathbf{M} \right)_{ij}^{\alpha\beta} = \delta_{\alpha\beta} \delta_{ij} + \delta_{\alpha i} \delta_{\beta j}, \quad (\text{A5})$$

where $\alpha, \beta = 1, 2, 3$ and $i, j = 1, 2, 3$ are color and flavor indices, respectively.

Inserting (A2) and (A3) and (A4) into $S_{11}(q)$, we get up to second order in m :

$$\begin{aligned} S_{11}(q) &\approx \left\{ (\gamma \cdot q + \mu \gamma^0) - m - \mathbf{M}^\dagger \frac{\gamma \cdot q - \mu \gamma^0}{(q_0 - \mu)^2 - |\mathbf{q}|^2 - m^2} \mathbf{M} \left(|G(q)|^2 \Lambda^+(\mathbf{q}) + |\bar{G}(q)|^2 \Lambda^-(\mathbf{q}) \right) \right. \\ &\quad \left. + \mathbf{M}^\dagger m \frac{G^*(q) \bar{G}(q) \Lambda^-(\mathbf{q}) + \bar{G}^*(q) G(q) \Lambda^+(\mathbf{q})}{(q_0 - \mu)^2 - |\mathbf{q}|^2 - m^2} \mathbf{M} \right\}^{-1} \\ &= \left\{ (\gamma \cdot q - \mu \gamma^0)(\gamma \cdot q + \mu \gamma^0) \right. \\ &\quad \left. - \left(\mathbf{M}^\dagger \mathbf{M} + \frac{\mathbf{M}^\dagger m^2 \mathbf{M}}{(q_0 - \mu)^2 - |\mathbf{q}|^2} \right) \left(|G(q)|^2 \Lambda^+(\mathbf{q}) + |\bar{G}(q)|^2 \Lambda^-(\mathbf{q}) \right) \right. \\ &\quad \left. - (\gamma \cdot q - \mu \gamma^0) \left(m - \mathbf{M}^\dagger m \mathbf{M} \frac{G^*(q) \bar{G}(q) \Lambda^-(\mathbf{q}) + \bar{G}^*(q) G(q) \Lambda^+(\mathbf{q})}{(q_0 - \mu)^2 - |\mathbf{q}|^2} \right) \right\}^{-1} \\ &\quad \times (\gamma \cdot q - \mu \gamma^0). \end{aligned} \quad (\text{A6})$$

Using

$$(\gamma \cdot q - \mu \gamma^0)(\gamma \cdot q + \mu \gamma^0) = \{q_0^2 - (\mu - |\mathbf{q}|)^2\} \Lambda^+(\mathbf{q}) + \{q_0^2 - (\mu + |\mathbf{q}|)^2\} \Lambda^-(\mathbf{q}) ,$$

we can transform (A6) into

$$\begin{aligned} S_{11}(q) = & \left\{ \Lambda^+(\mathbf{q}) \left[q_0^2 - (\mu - |\mathbf{q}|)^2 - \left(\mathbf{M}^\dagger \mathbf{M} + \frac{\mathbf{M}^\dagger m^2 \mathbf{M}}{(q_0 - \mu)^2 - |\mathbf{q}|^2} \right) |G(q)|^2 \right] \Lambda^+(\mathbf{q}) \right. \\ & + \Lambda^-(\mathbf{q}) \left[q_0^2 - (\mu + |\mathbf{q}|)^2 - \left(\mathbf{M}^\dagger \mathbf{M} + \frac{\mathbf{M}^\dagger m^2 \mathbf{M}}{(q_0 - \mu)^2 - |\mathbf{q}|^2} \right) |\overline{G}(q)|^2 \right] \Lambda^-(\mathbf{q}) \\ & - \Lambda^+(\mathbf{q}) \gamma^0 [q^0 - \mu + |\mathbf{q}|] \left(m - \mathbf{M}^\dagger m \mathbf{M} \frac{G^*(q) \overline{G}(q)}{(q_0 - \mu)^2 - |\mathbf{q}|^2} \right) \Lambda^-(\mathbf{q}) \\ & \left. - \Lambda^-(\mathbf{q}) \gamma^0 [q^0 - \mu - |\mathbf{q}|] \left(m - \mathbf{M}^\dagger m \mathbf{M} \frac{\overline{G}^*(q) G(q)}{(q_0 - \mu)^2 - |\mathbf{q}|^2} \right) \Lambda^+(\mathbf{q}) \right\}^{-1} \\ & \times \gamma^0 (q_0 - \mu - \boldsymbol{\alpha} \cdot \mathbf{q}) . \end{aligned} \quad (\text{A7})$$

Note that (A7) has the structure

$$\begin{aligned} S_{11}(q) &= \{ \Lambda^+ A \Lambda^+ + \Lambda^- D \Lambda^- + \Lambda^+ B \Lambda^- + \Lambda^- C \Lambda^+ \}^{-1} \gamma^0 (q_0 - \mu - \boldsymbol{\alpha} \cdot \mathbf{q}) \\ &\equiv \{ F \}^{-1} \gamma^0 (q_0 - \mu - \boldsymbol{\alpha} \cdot \mathbf{q}) \end{aligned} \quad (\text{A8})$$

with

$$\begin{aligned} A &= q_0^2 - \epsilon_q^2 - \mathbf{M}^\dagger m^2 \mathbf{M} \frac{|G(q)|^2}{(q_0 - \mu)^2 - |\mathbf{q}|^2} , \\ D &= q_0^2 - \overline{\epsilon}_q^2 - \mathbf{M}^\dagger m^2 \mathbf{M} \frac{|\overline{G}(q)|^2}{(q_0 - \mu)^2 - |\mathbf{q}|^2} , \\ B &= -\gamma^0 [q_0 - \mu + |\mathbf{q}|] \left(m - \mathbf{M}^\dagger m \mathbf{M} \frac{G^*(q) \overline{G}(q)}{(q_0 - \mu)^2 - |\mathbf{q}|^2} \right) , \\ C &= -\gamma^0 [q_0 - \mu - |\mathbf{q}|] \left(m - \mathbf{M}^\dagger m \mathbf{M} \frac{\overline{G}^*(q) G(q)}{(q_0 - \mu)^2 - |\mathbf{q}|^2} \right) , \end{aligned} \quad (\text{A9})$$

where

$$\epsilon_q \equiv (\mu - |\mathbf{q}|)^2 + \mathbf{M}^\dagger \mathbf{M} |G(q)|^2 , \quad (\text{A10})$$

$$\overline{\epsilon}_q \equiv (\mu + |\mathbf{q}|)^2 + \mathbf{M}^\dagger \mathbf{M} |\overline{G}(q)|^2 . \quad (\text{A11})$$

Here the projectors Λ^\pm are short for $\Lambda^\pm(\mathbf{q})$, and satisfy $\Lambda^\pm \Lambda^\pm = \Lambda^\pm$ and $\Lambda^+ + \Lambda^- = \mathbf{1}$, where the unit matrix refers to the Dirac space.

We will use now that the inverse of

$$F \equiv \Lambda^+ A \Lambda^+ + \Lambda^+ B \Lambda^- + \Lambda^- C \Lambda^+ + \Lambda^- D \Lambda^-$$

reads

$$\begin{aligned}
F^{-1} &= \Lambda^+ A^{-1} \Lambda^+ + \Lambda^- D^{-1} \Lambda^- \\
&\quad - \Lambda^+ A^{-1} B D^{-1} \Lambda^- - \Lambda^- D^{-1} C A^{-1} \Lambda^+ \\
&\quad + \Lambda^+ A^{-1} B D^{-1} C A^{-1} \Lambda^+ + \Lambda^- D^{-1} C A^{-1} B D^{-1} \Lambda^- \\
&\quad + \mathcal{O}(m^3)
\end{aligned}$$

and furthermore that $\gamma^0 \Lambda^\pm = \Lambda^\mp \gamma^0$ and $\Lambda^\pm(\mathbf{q}) \boldsymbol{\alpha} \cdot \mathbf{q} = \pm |\mathbf{q}| \Lambda^\pm(\mathbf{q})$. Then, we have

$$\begin{aligned}
S_{11}(q) &\approx \frac{\gamma^0 \Lambda^-(\mathbf{q})(q_0 - \mu + |\mathbf{q}|)}{q_0^2 - \epsilon_q^2} + \frac{\gamma^0 \Lambda^+(\mathbf{q})(q_0 - \mu - |\mathbf{q}|)}{q_0^2 - \bar{\epsilon}_q^2} \\
&\quad + \left((q_0 - \mu)^2 - |\mathbf{q}|^2 \right) \left\{ \frac{1}{q_0^2 - \epsilon_q^2} m \frac{1}{q_0^2 - \bar{\epsilon}_q^2} \Lambda^+(\mathbf{q}) + \frac{1}{q_0^2 - \bar{\epsilon}_q^2} m \frac{1}{q_0^2 - \epsilon_q^2} \Lambda^-(\mathbf{q}) \right\} \\
&\quad - G^*(q) \bar{G}(q) \frac{1}{q_0^2 - \epsilon_q^2} \mathbf{M}^\dagger m \mathbf{M} \frac{1}{q_0^2 - \bar{\epsilon}_q^2} \Lambda^+(\mathbf{q}) \\
&\quad - \bar{G}^*(q) G(q) \frac{1}{q_0^2 - \bar{\epsilon}_q^2} \mathbf{M}^\dagger m \mathbf{M} \frac{1}{q_0^2 - \epsilon_q^2} \Lambda^-(\mathbf{q}) \\
&\quad + \frac{1}{q_0^2 - \epsilon_q^2} \mathbf{M}^\dagger m^2 \mathbf{M} \frac{|G(q)|^2}{(q_0 - \mu)^2 - |\mathbf{q}|^2} \frac{\gamma^0 \Lambda^-(\mathbf{q})(q_0 - \mu + |\mathbf{q}|)}{q_0^2 - \epsilon_q^2} \\
&\quad + \frac{1}{q_0^2 - \bar{\epsilon}_q^2} \mathbf{M}^\dagger m^2 \mathbf{M} \frac{|\bar{G}(q)|^2}{(q_0 - \mu)^2 - |\mathbf{q}|^2} \frac{\gamma^0 \Lambda^+(\mathbf{q})(q_0 - \mu - |\mathbf{q}|)}{q_0^2 - \bar{\epsilon}_q^2} \\
&\quad + \frac{(q_0 - \mu)^2 - |\mathbf{q}|^2}{q_0^2 - \epsilon_q^2} \left(m - \mathbf{M}^\dagger m \mathbf{M} \frac{G^*(q) \bar{G}(q)}{(q_0 - \mu)^2 - |\mathbf{q}|^2} \right) \frac{1}{q_0^2 - \bar{\epsilon}_q^2} \\
&\quad \quad \times \left(m - \mathbf{M}^\dagger m \mathbf{M} \frac{\bar{G}^*(q) G(q)}{(q_0 - \mu)^2 - |\mathbf{q}|^2} \right) \frac{\gamma^0 \Lambda^-(\mathbf{q})(q_0 - \mu + |\mathbf{q}|)}{q_0^2 - \epsilon_q^2} \\
&\quad + \frac{(q_0 - \mu)^2 - |\mathbf{q}|^2}{q_0^2 - \bar{\epsilon}_q^2} \left(m - \mathbf{M}^\dagger m \mathbf{M} \frac{\bar{G}^*(q) G(q)}{(q_0 - \mu)^2 - |\mathbf{q}|^2} \right) \frac{1}{q_0^2 - \epsilon_q^2} \\
&\quad \quad \times \left(m - \mathbf{M}^\dagger m \mathbf{M} \frac{G^*(q) \bar{G}(q)}{(q_0 - \mu)^2 - |\mathbf{q}|^2} \right) \frac{\gamma^0 \Lambda^+(\mathbf{q})(q_0 - \mu - |\mathbf{q}|)}{q_0^2 - \bar{\epsilon}_q^2} \\
&\quad + \mathcal{O}(m^3) .
\end{aligned} \tag{A12}$$

We apply now the following approximations

$$\begin{aligned}
\epsilon_q^2 &= (\mu - |\mathbf{q}|)^2 + \mathbf{M}^\dagger \mathbf{M} |G(q)|^2 \approx (\mu - |\mathbf{q}|)^2 + |G(q)|^2 \equiv \epsilon_q^2 , \\
\bar{\epsilon}_q^2 &= (\mu + |\mathbf{q}|)^2 + \mathbf{M}^\dagger \mathbf{M} |\bar{G}(q)|^2 \approx (\mu + |\mathbf{q}|)^2 + |\bar{G}(q)|^2 \equiv \bar{\epsilon}_q^2 ,
\end{aligned} \tag{A13}$$

and, since $|\mathbf{q}| \approx \mu + q_{||}$,

$$\epsilon_q^2 \approx q_{||}^2 + |G(q)|^2 , \tag{A14}$$

$$\bar{\epsilon}_q^2 \approx 4\mu^2 , \tag{A15}$$

$$(q_0 - \mu)^2 - |\mathbf{q}|^2 \approx -2\mu(q_0 + q_{||}) . \tag{A16}$$

Then equation (A12) simplifies to

$$\begin{aligned}
S_{11}(q) = & \gamma^0 \frac{q_0 + q_{||}}{q_0^2 - \epsilon_q^2} \Lambda^-(\mathbf{q}) + \frac{\gamma^0 \Lambda^+(\mathbf{q})}{2\mu} + \frac{m}{2\mu} \frac{q_0 + q_{||}}{q_0^2 - \epsilon_q^2} \\
& + \gamma^0 \frac{m^2}{2\mu} \left(\frac{q_0 + q_{||}}{q_0^2 - \epsilon_q^2} \right)^2 \Lambda^-(\mathbf{q}) - \gamma^0 \frac{\mathbf{M}^\dagger m^2 \mathbf{M}}{2\mu} \left(\frac{|G(q)|}{q_0^2 - \epsilon_q^2} \right)^2 \Lambda^-(\mathbf{q}) \\
& + \mathcal{O} \left(\mu^{-2}, m^3, |G(q)|^2 \frac{\mathbf{M}^\dagger \mathbf{M} - \mathbf{1}}{(q_0^2 - \epsilon_q^2)^2} \right). \tag{A17}
\end{aligned}$$

Note that $S_{22}(q)$ follows from (A12) under the substitutions

$$\Lambda^\pm(\mathbf{q}) \leftrightarrow \Lambda^\mp(\mathbf{q}), \quad \pm\mu \leftrightarrow \mp\mu, \quad \pm|\mathbf{q}| \leftrightarrow \mp|\mathbf{q}|, \quad \pm G^* \leftrightarrow \mp G, \quad \pm \overline{G}^* \leftrightarrow \mp \overline{G}, \quad \text{and } \mathbf{M}^\dagger \leftrightarrow \mathbf{M}, \tag{A18}$$

which also imply $\pm q_{||} \leftrightarrow \mp q_{||}$. In fact, these rules can be traced back to the replacements $G_0^+(q) \leftrightarrow G_0^-(q)$ and $\Delta(q) \leftrightarrow \gamma^0 \Delta^\dagger(q) \gamma^0$ which link the various Nambu-Gorkov components in (A1) to each other. Using (A15) and

$$(q_0 + \mu)^2 - |\mathbf{q}|^2 \approx 2\mu(q_0 - q_{||}), \tag{A19}$$

we get

$$\begin{aligned}
S_{22}(q) = & \frac{\gamma^0 \Lambda^+(\mathbf{q})(q_0 - q_{||})}{q_0^2 - \epsilon_q^2} - \frac{\gamma^0 \Lambda^-(\mathbf{q})}{2\mu} - \frac{m}{2\mu} \frac{q_0 - q_{||}}{q_0^2 - \epsilon_q^2} \\
& - \gamma^0 \frac{m^2}{2\mu} \left(\frac{q_0 - q_{||}}{q_0^2 - \epsilon_q^2} \right)^2 \Lambda^+(\mathbf{q}) + \gamma^0 \frac{\mathbf{M} m^2 \mathbf{M}^\dagger}{2\mu} \left(\frac{|G(q)|}{q_0^2 - \epsilon_q^2} \right)^2 \Lambda^+(\mathbf{q}) \\
& + \mathcal{O} \left(\mu^{-2}, m^3, |G(q)|^2 \frac{\mathbf{M}^\dagger \mathbf{M} - \mathbf{1}}{(q_0^2 - \epsilon_q^2)^2} \right). \tag{A20}
\end{aligned}$$

Finally,

$$\begin{aligned}
S_{21}(q) = & -G_0^-(q) \Delta(q) S_{11}(q) \tag{A21} \\
= & -\frac{\gamma^0(q_0 - \mu - \boldsymbol{\alpha} \cdot \mathbf{q}) + m}{(q_0 - \mu)^2 - |\mathbf{q}|^2 - m^2} \times \mathbf{M} \left[G(q) \Lambda^+(\mathbf{q}) + \overline{G}(q) \Lambda^-(\mathbf{q}) \right] \times S_{11}(q) \\
= & + \left[\frac{q_0 - \mu - |\mathbf{q}|}{(q_0 - \mu)^2 - |\mathbf{q}|^2} \mathbf{M} G(q) \Lambda^-(\mathbf{q}) + \frac{q_0 - \mu + |\mathbf{q}|}{(q_0 - \mu)^2 - |\mathbf{q}|^2} \mathbf{M} \overline{G}(q) \Lambda^+(\mathbf{q}) \right] \gamma^0 S_{11}(q) \\
& - \frac{m}{(q_0 - \mu)^2 - |\mathbf{q}|^2} \mathbf{M} \left[G(q) \Lambda^+(\mathbf{q}) + \overline{G}(q) \Lambda^-(\mathbf{q}) \right] S_{11}(q) \\
& + m^2 \left[\frac{q_0 - \mu - |\mathbf{q}|}{((q_0 - \mu)^2 - |\mathbf{q}|^2)^2} \mathbf{M} G(q) \Lambda^-(\mathbf{q}) + \frac{q_0 - \mu + |\mathbf{q}|}{(q_0 - \mu)^2 - |\mathbf{q}|^2} \mathbf{M} \overline{G}(q) \Lambda^+(\mathbf{q}) \right] \\
& \times \gamma^0 S_{11}(q) + \mathcal{O}(m^3) \\
= & \frac{\mathbf{M} G(q) \Lambda^-(\mathbf{q})}{q_0^2 - \epsilon_q^2} - \gamma^0 \frac{\mathbf{M} m}{2\mu} \frac{G(q) \Lambda^+(\mathbf{q})}{q_0^2 - \epsilon_q^2} - \gamma^0 \frac{m \mathbf{M}}{2\mu} \frac{G(q) \Lambda^-(\mathbf{q})}{q_0^2 - \epsilon_q^2} \\
& + \frac{\mathbf{M} m^2}{2\mu} \frac{G(q) (q_0 + q_{||}) \Lambda^-(\mathbf{q})}{(q_0^2 - \epsilon_q^2)^2} - \frac{\mathbf{M} \mathbf{M}^\dagger m^2 \mathbf{M}}{2\mu} \frac{G(q) |G(q)|^2 \Lambda^-(\mathbf{q})}{(q_0 + q_{||}) (q_0^2 - \epsilon_q^2)^2} \\
& - \frac{m^2}{2\mu} \frac{\mathbf{M} G(q) \Lambda^-(\mathbf{q})}{(q_0 + q_{||}) (q_0^2 - \epsilon_q^2)} + \mathcal{O} \left(\mu^{-2}, m^3, |G(q)|^2 \frac{\mathbf{M}^\dagger \mathbf{M} - \mathbf{1}}{(q_0^2 - \epsilon_q^2)^2} \right).
\end{aligned}$$

The latter equation can be simplified to

$$\begin{aligned}
S_{21}(q) = & \frac{\mathbf{M}G(q)\Lambda^-(\mathbf{q})}{q_0^2 - \epsilon_q^2} - \gamma^0 \frac{\mathbf{M}m}{2\mu} \frac{G(q)\Lambda^+(\mathbf{q})}{q_0^2 - \epsilon_q^2} - \gamma^0 \frac{m\mathbf{M}}{2\mu} \frac{G(q)\Lambda^-(\mathbf{q})}{q_0^2 - \epsilon_q^2} \\
& + \frac{1}{2\mu} \left\{ \mathbf{M}m^2 (q_0 + q_{||}) - m^2 \mathbf{M} (q_0 - q_{||}) \right\} \frac{G(q)\Lambda^-(\mathbf{q})}{(q_0^2 - \epsilon_q^2)^2} \\
& + \mathcal{O} \left(\mu^{-2}, m^3, |G(q)|^2 \frac{\mathbf{M}^\dagger \mathbf{M} - 1}{(q_0^2 - \epsilon_q^2)^2} \right). \tag{A22}
\end{aligned}$$

Again, S_{12} follows under the substitutions (A18) from S_{21} . Using (A15) and (A19), we get

$$\begin{aligned}
S_{12}(q) = & -\frac{\mathbf{M}^\dagger G^*(q)\Lambda^+(\mathbf{q})}{q_0^2 - \epsilon_q^2} - \gamma^0 \frac{\mathbf{M}^\dagger m}{2\mu} \frac{G^*(q)\Lambda^-(\mathbf{q})}{q_0^2 - \epsilon_q^2} - \gamma^0 \frac{m\mathbf{M}^\dagger}{2\mu} \frac{G^*(q)\Lambda^+(\mathbf{q})}{q_0^2 - \epsilon_q^2} \\
& + \frac{1}{2\mu} \left\{ \mathbf{M}^\dagger m^2 (q_0 - q_{||}) - m^2 \mathbf{M}^\dagger (q_0 + q_{||}) \right\} \frac{G^*(q)\Lambda^+(\mathbf{q})}{(q_0^2 - \epsilon_q^2)^2} \\
& + \mathcal{O} \left(\mu^{-2}, m^3, |G(q)|^2 \frac{\mathbf{M}^\dagger \mathbf{M} - 1}{(q_0^2 - \epsilon_q^2)^2} \right). \tag{A23}
\end{aligned}$$

Note that the above determined quark propagators (A17), (A20), (A22) and (A23) show neither a $\overline{G}(q)$ nor a $\overline{G}^*(q)$ dependence. In fact, such terms first arise at order $\mathcal{O}(\mu^{-2})$.

2. Perturbative calculation of the mass corrections (2) to the propagator (1):

As a check on the precedent analysis, we now carry a mass perturbation analysis of the quark propagator in the CFL phase. We recall that the massless propagator reads [9] ^{#12}

$$\begin{aligned}
S_{11}(q) &= \left[\Lambda^+(\mathbf{q}) \gamma^0 \frac{q_0 - \mu + |\mathbf{q}|}{q_0^2 - \epsilon_q^2} \Lambda^-(\mathbf{q}) + \Lambda^-(\mathbf{q}) \gamma^0 \frac{q_0 - \mu - |\mathbf{q}|}{q_0^2 - \bar{\epsilon}_q^2} \Lambda^+(\mathbf{q}) \right], \\
S_{12}(q) &= - \left[\Lambda^+(\mathbf{q}) \mathbf{M}^\dagger \frac{G^*(q)}{q_0^2 - \bar{\epsilon}_q^2} \Lambda^+(\mathbf{q}) + \Lambda^-(\mathbf{q}) \mathbf{M}^\dagger \frac{\overline{G}^*(q)}{q_0^2 - \bar{\epsilon}_q^2} \Lambda^-(\mathbf{q}) \right], \\
S_{21}(q) &= \left[\Lambda^-(\mathbf{q}) \mathbf{M} \frac{G(q)}{q_0^2 - \epsilon_q^2} \Lambda^-(\mathbf{q}) + \Lambda^+(\mathbf{q}) \mathbf{M} \frac{\overline{G}(q)}{q_0^2 - \epsilon_q^2} \Lambda^+(\mathbf{q}) \right], \\
S_{22}(q) &= \left[\Lambda^-(\mathbf{q}) \gamma^0 \frac{q_0 + \mu - |\mathbf{q}|}{q_0^2 - \epsilon_q^2} \Lambda^+(\mathbf{q}) + \Lambda^+(\mathbf{q}) \gamma^0 \frac{q_0 + \mu + |\mathbf{q}|}{q_0^2 - \bar{\epsilon}_q^2} \Lambda^-(\mathbf{q}) \right] \tag{A24}
\end{aligned}$$

with $\epsilon_q^2 = (\mu - |\mathbf{q}|)^2 + \mathbf{M}^\dagger \mathbf{M} |G(q)|^2$ and $\bar{\epsilon}_q^2 = (\mu + |\mathbf{q}|)^2 + \mathbf{M}^\dagger \mathbf{M} |\overline{G}(q)|^2$. Using (A24), we can calculate the mass corrections in perturbation theory, i.e.

$$\Delta_m \mathbf{S}(q) = \mathbf{S}(q) \begin{pmatrix} m & 0 \\ 0 & m \end{pmatrix} \mathbf{S}(q), \tag{A25}$$

$$\Delta_{m^2} \mathbf{S}(q) = \mathbf{S}(q) \begin{pmatrix} m & 0 \\ 0 & m \end{pmatrix} \mathbf{S}(q) \begin{pmatrix} m & 0 \\ 0 & m \end{pmatrix} \mathbf{S}(q), \tag{A26}$$

^{#12}These expressions can easily be derived with the methods of the former section. Especially, they are consistent with (A17), (A20), (A22) and (A23) to order $\mathcal{O}(m^0, \mu^{-1})$ and under the approximations (A14), (A15), (A16) and (A19).

etc., where, in general, $m = \text{diag}(m_u, m_d, m_s)$. The remaining task is just to insert the terms (A24) into (A25) and (A26). One can easily check that the m and m^2 terms of (A17), (A20), (A22) and (A23) are recovered in this way. Hence, the direct and perturbative arguments give the same result to the order quoted. In retrospect, this is not surprising. Both approaches use the Dyson expansion of the propagator. In the perturbative argument, the full massive propagator is expanded in terms of the full massless propagator. In the direct approach, the same expansion is performed on the level of the free propagators. The gap functions $\mathbf{M}G(q)$ and $\mathbf{M}\overline{G}(q)$ are completely passive with respect to these expansions. Therefore the results are the same.

The neglect of the color-flavor non-diagonal terms in (A5) through the approximation (A13) which has also been used in [9] to simplify the denominators, can be justified as follows. The eigenvalues of \mathbf{M} ($=\mathbf{M}^\dagger$) read [12]

$$\text{eig}(\mathbf{M}) = +2, +1, +1, +1, -1, -1, -1, -1, -1 .$$

Thus the eigenvalues of $\mathbf{M}^\dagger\mathbf{M} = \mathbf{M}^2$ are ^{#13}

$$\text{eig}(\mathbf{M}^\dagger\mathbf{M}) = 4, 1, 1, 1, 1, 1, 1, 1, 1 .$$

Note that eight eigenvalues are equal to unit and only the ninth deviates from this value [21]. This is related to an explicit U(1) degree of freedom in the U(3) color-flavor phase, whereas the agreement of the other eight eigenvalues corresponds to the SU(3) sector in the color-flavor phase. Throughout, we have specialized to the SU(3) phase as indicated in the introduction, leaving the issue of the additional U(1) in the presence of the triangle anomaly for a future discussion.

3. Derivation of the mass formula of the generalized Goldstone meson:

Following Ref. [9], we consider the chiral Ward identity implied by the underlying flavor symmetry in the CFL phase. Indeed, when chiral symmetry is softly broken by massive quarks $m = \text{diag}(m_u, m_d, m_s)$, then the pions are expected to be massive. Hence

$$0 \equiv \int d^4x \partial_x^\mu \left\langle \text{BCS} \left| T^* \mathbf{A}_\mu^\alpha(x) \boldsymbol{\pi}_B^\beta(0) \right| \text{BCS} \right\rangle , \quad (\text{A27})$$

where the axial-vector current \mathbf{A}_μ^a is given in (A54) and the pion field $\boldsymbol{\pi}_B(x)$ in the CFL phase is defined as (see Appendix-7)

$$\boldsymbol{\pi}_B^\beta(x) = \begin{pmatrix} 0 & \overline{\psi} \gamma^0 (\mathbf{M} i \tau^\beta \gamma_5)^\dagger \gamma^0 \psi_C(x) \\ \overline{\psi}_C \mathbf{M} i \tau^\beta \gamma_5 \psi(x) & 0 \end{pmatrix} , \quad (\text{A28})$$

^{#13}For the general case $N_c = N_f$, the “+2” and “4” have to be replaced by $N_c - 1$ and $(N_c - 1)^2$, respectively. Furthermore, there are $\frac{1}{2}N_c(N_c - 1)$ eigenvalues +1 and $\frac{1}{2}N_c(N_c + 1) - 1$ eigenvalues -1.

which is consistent with (12). The flavor axial-vector current in the CFL phase (see Appendix-6) obeys the local divergence equation

$$\partial \cdot \mathbf{A}^\alpha(x) = \begin{pmatrix} \bar{\psi} i \left[m, \frac{1}{2} \tau^\alpha \right]_+ \gamma_5 \psi(x) & 0 \\ 0 & \bar{\psi}_C i \left[m, \frac{1}{2} \tau^{\alpha*} \right]_+ \gamma_5 \psi_C(x) \end{pmatrix}. \quad (\text{A29})$$

For massless quarks, the hermitean axial-isovector charge

$$\mathbf{Q}_5^\alpha \equiv \mathbf{Q}_5^\alpha(x^0) = \int d^3x \begin{pmatrix} \bar{\psi} \frac{1}{2} \tau^\alpha \gamma^0 \gamma_5 \psi(x) & 0 \\ 0 & \bar{\psi}_C \frac{1}{2} \tau^{\alpha*} \gamma^0 \gamma_5 \psi_C(x) \end{pmatrix} \quad (\text{A30})$$

is conserved and generates axial-vector rotations, e.g.

$$[\mathbf{Q}_5^\alpha, \Psi(x)] = -\gamma_5 \frac{1}{2} \mathbf{T}^\alpha \Psi(x). \quad (\text{A31})$$

In terms of (A29-A31), the identity (A28) yields the axial Ward-identity

$$\int d^4x \left\langle \text{BCS} \left| T^* \left[m, \frac{1}{2} \pi^\alpha(x) \right]_+ \pi_B^\beta(0) \right| \text{BCS} \right\rangle = \left\langle \text{BCS} \left| \Sigma_B^{\alpha\beta}(0) \right| \text{BCS} \right\rangle, \quad (\text{A32})$$

where the diquark field $\Sigma_B^{\alpha\beta}(x)$ is defined as

$$\Sigma^{\alpha\beta} = \bar{\Psi}(x) \left[\frac{1}{2} \mathbf{T}^\alpha, \begin{pmatrix} 0 & -i\tau^\beta \mathbf{M}^\dagger \\ i\mathbf{M}\tau^\beta & 0 \end{pmatrix} \right] \Psi(x) \quad (\text{A33})$$

and $\pi(x)$ is the diagonal pion field

$$\pi^\alpha(x) = \begin{pmatrix} \bar{\psi} i\tau^\alpha \gamma_5 \psi(x) & 0 \\ 0 & \bar{\psi}_C i\tau^{\alpha*} \gamma_5 \psi_C(x) \end{pmatrix}. \quad (\text{A34})$$

The nonconfining character of the weak coupling description allows for the occurrence of the gapped qq and/or $\bar{q}q$ exchange. Hence,

$$\begin{aligned} \left\langle \text{BCS} \left| \Sigma_B^{\alpha\beta}(0) \right| \text{BCS} \right\rangle &\approx -\int \frac{d^4q}{(2\pi)^4} \text{Tr} \left[i\gamma_5 \frac{1}{2} [m, \mathbf{T}^\alpha]_+ i\mathbf{S}(q) \mathbf{\Pi}_B^\beta i\mathbf{S}(q) \right] \\ &+ \left\{ \int \frac{d^4q}{(2\pi)^4} \text{Tr} \left[i\gamma_5 \frac{1}{2} [m, \mathbf{T}^\alpha]_+ i\mathbf{S}(q) i\mathbf{\Gamma}_\pi^\xi i\mathbf{S}(q) \right] \right\} \left(\frac{-i}{M^2} \right)^{\xi\xi'} \left\{ \int \frac{d^4q}{(2\pi)^4} \text{Tr} \left[i\mathbf{\Gamma}_\pi^{\xi'} i\mathbf{S}(q) \mathbf{\Pi}_B^\beta i\mathbf{S}(q) \right] \right\} \end{aligned} \quad (\text{A35})$$

with

$$\mathbf{\Pi}_B^\beta \equiv \begin{pmatrix} 0 & \gamma^0 (i\mathbf{M}\tau^\beta \gamma_5)^\dagger \gamma^0 \\ i\mathbf{M}\tau^\beta \gamma_5 & 0 \end{pmatrix}. \quad (\text{A36})$$

In the chiral limit $m_i \rightarrow 0$, $i \in \{u, d, s\}$, the first term in (A35) drops out and the identity is fulfilled if $1/M^2$ is sufficiently singular in m_i to match the numerator. The traces can be evaluated in weak coupling. The result is ^{#14}

$$\int \frac{d^4q}{(2\pi)^4} \text{Tr} \left[i\gamma_5 \frac{1}{2} [m, \mathbf{T}^\alpha]_+ i\mathbf{S}(q) i\mathbf{\Gamma}_\pi^\xi i\mathbf{S}(q) \right] = \mathcal{O}(m^2), \quad (\text{A37})$$

$$\int \frac{d^4q}{(2\pi)^4} \text{Tr} \left[i\mathbf{\Gamma}_\pi^{\xi'} i\mathbf{S}(q) \mathbf{\Pi}_B^\beta i\mathbf{S}(q) \right] = \delta^{\xi'\beta} \frac{16i}{F_T} \int \frac{d^4q}{(2\pi)^4} \frac{G(q)}{q_0^2 - \epsilon_q^2}, \quad (\text{A38})$$

^{#14}The use of F_T instead of F_S in the pion vertex follows from the fact that the intermediate BCS pion is generated by a chiral rotation of the BCS ground state. A similar interpretation in matter is made in [24].

which shows that $M^2 = \mathcal{O}(m^2)$. To determine the coefficient, we need to expand the vertices and the propagators in (A35) to leading order in m . The $\mathcal{O}(m)$ corrections to both $G(p)$ and $\Gamma(p)$ do not contribute. They trace to zero because of a poor spin structure. Therefore, only the $\mathcal{O}(m)$ correction to the propagator (1) is needed, i.e. (2). Inserting (1) *together* with the mass correction (2) into (A37) yields

$$\begin{aligned} & \int \frac{d^4 q}{(2\pi)^4} \text{Tr} \left[i\gamma_5 \frac{1}{2} [m, \mathbf{T}^\alpha]_+ i\mathbf{S}(q) i\mathbf{\Gamma}_\pi^\xi i\mathbf{S}(q) \right] \\ &= \frac{\mu G_0}{8\pi^2 F_T} \text{Tr}_{cf} \left([m^2, \tau^\alpha] \left(\mathbf{M}^\dagger \mathbf{M}^\beta - \mathbf{M}^{\beta\dagger} \mathbf{M} \right) + [m^2, \tau^{\alpha*}] \left(\mathbf{M} \mathbf{M}^{\beta\dagger} - \mathbf{M}^\beta \mathbf{M}^\dagger \right) \right). \end{aligned} \quad (\text{A39})$$

Here, the resulting integral simplifies under a contour integration in the following way:

$$\begin{aligned} i \int \frac{d^4 q}{(2\pi)^4} \frac{q_0 \pm q_{||}}{(q_0^2 - \epsilon_q^2)^2} \frac{|G(q_{||})|^2}{2\mu F_T} &= i2\pi \int_0^{2\mu} \frac{dq_\perp q_\perp}{(2\pi)^2} \int_{-\infty}^{\infty} \frac{dq_{||}}{2\pi} \frac{|G(q_{||})|^2}{2\mu F_T} \int \frac{idq_4}{2\pi} \frac{iq_4 \pm q_{||}}{(q_4^2 + \epsilon_q^2)^2} \\ &= \mp \frac{\mu^2}{\pi^2} \int_0^{\infty} dq_{||} \frac{|G(q_{||})|^2}{2\mu F_T} \frac{q_{||}}{4\epsilon_q^3} \approx \mp \frac{\mu}{8\pi^2 F_T} \int_{G_0}^{\Lambda_*} dq_{||} \frac{|G(q_{||})|^2}{q_{||}^2} \\ &\approx \mp \frac{\mu}{8\pi^2 F_T} \int_0^{x_0} dx \frac{e^x}{\Lambda_*} G_0^2 \sin^2 \left(\frac{\pi x}{2x_0} \right) \\ &\approx \mp \frac{\mu}{8\pi^2 F_T} \frac{G_0^2}{\Lambda_*} e^{x_0} = \mp \frac{\mu}{8\pi^2 F_T} G_0, \end{aligned}$$

where the gap solution (6) and the logarithmic scales $x = \ln(\Lambda_*/q_{||})$ and $x_0 = \ln(\Lambda_*/G_0)$ were inserted in the second to last line. Furthermore, $[m, [m, \tau^\alpha]_+] = [m^2, \tau^\alpha]$ was used.

Inserting (A38) and (A39) in (A35) and noting that

$$\langle \Sigma_B^{\alpha\beta} \rangle \equiv \text{Tr} \left(\left[\frac{1}{2} \mathbf{T}^\alpha, \begin{pmatrix} 0 & -i\tau^\beta \mathbf{M}^\dagger \\ i\mathbf{M} \tau^\beta & 0 \end{pmatrix} \right]_+ i\mathbf{S} \right) = -8\delta^{\alpha\beta} \int \frac{d^4 q}{(2\pi)^4} \frac{G(q)}{q_0^2 - \epsilon_q^2}, \quad (\text{A40})$$

we obtain for the mass of the Goldstone modes

$$(M^2)^{\alpha\beta} \approx -\frac{\mu G_0}{4\pi^2 F_T^2} \text{Tr}_{cf} \left([m^2, \tau^\alpha] \left(\mathbf{M}^\dagger \mathbf{M}^\beta - \mathbf{M}^{\beta\dagger} \mathbf{M} \right) + [m^2, \tau^{\alpha*}] \left(\mathbf{M} \mathbf{M}^{\beta\dagger} - \mathbf{M}^\beta \mathbf{M}^\dagger \right) \right), \quad (\text{A41})$$

which is (21), see also Ref. [9]. Note that the color-flavor traces, which first appeared in the transition from (A37) to (A39), yield zero.

In order to get a non-zero result for the mass matrix of the generalized pion, we have to insert in (A37) the next-to-leading order, $\mathcal{O}(1/\mu)$, even for the massless terms of the propagator, i.e. the second terms on the right hand sides of (A17) and (A20) which can be traced back to the leading terms of the antiparticle propagator, see (A24) ^{#15}. These terms are in fact antiparticle-gap *independent*. The first antiparticle-gap *dependent* piece appears

^{#15}The $1/\mu$ expansion of the numerators and denominators of the particle propagators only modifies the leading result (A39) by overall factors that do not prevent the vanishing of the color-flavor traces.

at order $\mathcal{O}(1/\mu^2)$ and is therefore subleading. This is fortunate, since according to [15] the antiparticle-gap is gauge-fixing-term dependent. Inserting the above mentioned terms in (A37), we get

$$\begin{aligned}
(A37) &= (A39) + \frac{i}{4\mu^2 F_T} \int \frac{d^4 q}{(2\pi)^4} \frac{|G(q)|^2}{q_0^2 - \epsilon_q^2} \\
&\quad \times \left\{ \text{Tr}_{cf} \left([m, \tau^\alpha]_+ \left(\mathbf{M}^{\xi\dagger} m \mathbf{M} + \mathbf{M}^\dagger m \mathbf{M}^\xi \right) \right) \right. \\
&\quad \left. + \text{Tr}_{cf} \left([m, \tau^{\alpha*}]_+ \left(\mathbf{M}^\xi m \mathbf{M}^\dagger + \mathbf{M} m \mathbf{M}^{\xi\dagger} \right) \right) \right\}. \quad (A42)
\end{aligned}$$

Note that

$$\begin{aligned}
i \int \frac{d^4 q}{(2\pi)^4} \frac{|G(q)|^2}{q_0^2 - \epsilon_q^2} &= i 2\pi \int_0^{2\mu} \frac{dq_\perp q_\perp}{(2\pi)^2} \int_{-\infty}^{\infty} \frac{dq_\parallel}{2\pi} |G(q_\parallel)|^2 \int \frac{idq_4}{2\pi} \frac{-1}{q_4^2 + \epsilon_q^2} \\
&= \frac{\mu^2}{\pi^2} \int_0^\infty dq_\parallel \frac{|G(q_\parallel)|^2}{2\epsilon_q} \\
&\approx \frac{\mu^2}{2\pi^2} \int_{G_0}^{\Lambda_*} dq_\parallel \frac{|G(q_\parallel)|^2}{q_\parallel} \\
&= \frac{\mu^2}{2\pi^2} G_0^2 \int_0^{x_0} dx \sin^2 \left(\frac{\pi x}{2x_0} \right) \\
&= \frac{\mu^2}{2\pi^2} G_0^2 \frac{x_0}{2} = \frac{\mu^2 G_0^2 x_0}{4\pi^2}, \quad (A43)
\end{aligned}$$

where logarithmic scales $x = \ln(\Lambda_*/q_\parallel)$ and $x_0 = \ln(\Lambda_*/G_0)$ were used in the fourth line. Thus we have for $\Delta(A37) \equiv (A37) - (A39)$:

$$\begin{aligned}
\Delta(A37) &\approx \frac{G_0^2 x_0}{16\pi^2 F_T} \left\{ \text{Tr}_{cf} \left([m, \tau^\alpha]_+ \left(\mathbf{M}^{\xi\dagger} m \mathbf{M} + \mathbf{M}^\dagger m \mathbf{M}^\xi \right) \right) \right. \\
&\quad \left. + \text{Tr}_{cf} \left([m, \tau^{\alpha*}]_+ \left(\mathbf{M}^\xi m \mathbf{M}^\dagger + \mathbf{M} m \mathbf{M}^{\xi\dagger} \right) \right) \right\}. \quad (A44)
\end{aligned}$$

Since G_0 and F_T are of order $\mathcal{O}(\mu)$, we find that $\Delta(A37)$ is of order $\mathcal{O}(\mu)$. This means that the corresponding $(M^2)^{\alpha\beta}$ is of order $\mathcal{O}(\mu^0)$, since there is an additional $1/F_T$ factor from (A38), namely

$$\begin{aligned}
(M^2)^{\alpha\beta} &\approx -\frac{G_0^2 x_0}{8\pi^2 F_T^2} \left\{ \text{Tr}_{cf} \left([m, \tau^\alpha]_+ \left(\mathbf{M}^{\beta\dagger} m \mathbf{M} + \mathbf{M}^\dagger m \mathbf{M}^\beta \right) \right) \right. \\
&\quad \left. + \text{Tr}_{cf} \left([m, \tau^{\alpha*}]_+ \left(\mathbf{M}^\beta m \mathbf{M}^\dagger + \mathbf{M} m \mathbf{M}^{\beta\dagger} \right) \right) \right\}. \quad (A45)
\end{aligned}$$

In the flavor-symmetric case $m_u = m_d = m_s$ ($\equiv m_q$), the color-flavor traces simplify to

$$2m_q^2 \text{Tr}_{cf} \left(\tau^\alpha \left\{ \mathbf{M}^{\xi\dagger} \mathbf{M} + \mathbf{M}^\dagger \mathbf{M}^\xi \right\} \right) = 2m_q^2 \text{Tr}_{cf} \left(\tau^{\alpha*} \left\{ \mathbf{M}^\xi \mathbf{M}^\dagger + \mathbf{M} \mathbf{M}^{\xi\dagger} \right\} \right) = -16m_q^2 \delta^{\alpha\xi}.$$

The mass of the generalized pion at next-to-leading order now reads

$$\begin{aligned}
M^2 &\approx \frac{4G_0^2 x_0}{\pi^2 F_T^2} m_q^2 = \frac{4m_q^2}{\mu^2} \left\{ \frac{4\Lambda_\perp^6}{\pi m_E^5} \exp \left(\frac{-3\pi^2}{\sqrt{2}g} \right) \right\}^2 \frac{3\pi^2}{\sqrt{2}g} \\
&= \frac{2^{23} \pi^{10} m_q^2}{3^4 \sqrt{2} g^{11}} \exp \left(\frac{-3\sqrt{2}\pi^2}{g} \right), \quad (A46)
\end{aligned}$$

where we have used that $F_T = \mu/\pi$, eq. (7), $x_0 = \frac{\sqrt{3}\pi}{2h_*}$, eq. (8), $\Lambda_\perp = 2\mu$ and $m_E = \sqrt{\frac{N_f}{2}} \frac{g\mu}{\pi}$ with $N_f = 3$.

4. Proof of the color-identity (3):

Apply the standard identity for $SU(N_c)$ Gell-Mann matrices,

$$\sum_{a=1}^{N_c^2-1} \frac{1}{4} \lambda_{\alpha\beta}^a \lambda_{\gamma\delta}^a = \frac{1}{2} \delta_{\alpha\delta} \delta_{\gamma\beta} - \frac{1}{2N} \delta_{\alpha\beta} \delta_{\gamma\delta} , \quad (\text{A47})$$

to the expression $\sum_{a=1}^{N_c^2-1} \left(\frac{\lambda^{aT}}{2} \epsilon^A \frac{\lambda^a}{2} \right)_{\alpha\delta}$, i.e.

$$\begin{aligned} \sum_{a=1}^{N_c^2-1} \frac{1}{4} \lambda_{\alpha\beta}^{aT} \epsilon^{A\beta\gamma} \lambda_{\gamma\delta}^a &= \sum_{a=1}^{N_c^2-1} \frac{1}{4} \lambda_{\beta\alpha}^a \lambda_{\gamma\delta}^a \epsilon^{A\beta\gamma} = \left(\frac{1}{2} \delta_{\beta\delta} \delta_{\gamma\alpha} - \frac{1}{2N_c} \delta_{\beta\alpha} \delta_{\gamma\delta} \right) \epsilon^{A\beta\gamma} \\ &= \frac{1}{2} \left(\epsilon^{A\delta\alpha} - \frac{1}{N_c} \epsilon^{A\alpha\delta} \right) = -\frac{N_c+1}{2N_c} \epsilon^{A\alpha\delta} \end{aligned} \quad (\text{A48})$$

which is identical to (3) for the case $N_c = 3$. It is easy to check that also

$$\sum_a \frac{\lambda^a}{2} \epsilon_c^A \frac{\lambda^{aT}}{2} = -\frac{N_c+1}{2N_c} \epsilon_c^A \quad (\text{A49})$$

holds. Finally, by replacing $\beta \leftrightarrow \alpha$ in the bracket of the third term of (A48) one can easily derive

$$\sum_a \frac{\lambda^a}{2} \epsilon_c^A \frac{\lambda^a}{2} = -\frac{1}{2N_c} \epsilon_c^A . \quad (\text{A50})$$

5. Proof of the relations (14):

The first identity follows immediately from (3) or (A48), if one inserts

$$\begin{aligned} \sum_a \frac{\lambda^{aT}}{2} (\mathbf{M}^A) \frac{\lambda^a}{2} &= \sum_a \frac{\lambda^{aT}}{2} \left(\epsilon_f^I \epsilon_c^J \gamma_5 (\tau^A)^{IJ} \right) \frac{\lambda^a}{2} \\ &= -\frac{N_c+1}{2N_c} \left(\epsilon_f^I \epsilon_c^J \gamma_5 (\tau^A)^{IJ} \right) = -\frac{N_c+1}{2N_c} \mathbf{M}^A . \end{aligned} \quad (\text{A51})$$

It is easy to see that the same relation holds, if \mathbf{M}^A is replaced by $\mathbf{M}^{A\dagger}$.

In order to show the second relation of (14), we use that

$$\mathbf{M} \mathbf{M}^A \mathbf{M} = \gamma_5 \epsilon_f^I \epsilon_c^I \epsilon_f^J \left(\tau^A \right)^{JK} \epsilon_c^K \epsilon_f^L \epsilon_c^L$$

and that

$$\begin{aligned} \left(\epsilon_c^I \epsilon_c^K \epsilon_c^L \right)^{\alpha\beta} &= -\epsilon_c^{I\alpha\beta} \delta^{KL} + \epsilon_c^{I\alpha L} \delta^{K\beta} , \\ \left(\epsilon_f^I \epsilon_f^J \epsilon_f^L \right)^{ij} &= -\epsilon_f^{Lij} \delta^{IJ} + \epsilon_f^{LIj} \delta^{iJ} . \end{aligned}$$

Therefore

$$\begin{aligned} (\mathbf{M}\mathbf{M}^A\mathbf{M})^{\alpha i, \beta j} &= \gamma_5 \epsilon_f^{Kij} \epsilon_c^{J\alpha\beta} (\tau^A)^{JK} + \dots \\ &= \gamma_5 \epsilon_f^{Kij} \epsilon_c^{J\alpha\beta} (\tau^{AT})^{KJ} + \dots = (\mathbf{M}^{A\dagger})^{\alpha i, \beta j} + \dots, \end{aligned}$$

where the dots refer to terms which are symmetric in color-flavor and finally subleading to leading logarithm order. Naturally, also $(\mathbf{M}\mathbf{M}^{A\dagger}\mathbf{M}) = \mathbf{M}^A + \dots$ holds. Therefore the second relation of (14) approximately follows from the first one, if the above mentioned subleading terms are neglected.

6. The structure of the vector and axial-vector currents:

The two-component Nambu-Gorkov field

$$\Psi = \begin{pmatrix} \psi \\ C\bar{\psi}^T \end{pmatrix}$$

transforms under vector and axial-vector transformations as follows

$$\mathbf{U}_V \Psi = \begin{pmatrix} e^{i\frac{1}{2}\tau^A \alpha^A} & 0 \\ 0 & e^{-i\frac{1}{2}\tau^{A*} \alpha^A} \end{pmatrix} \Psi \quad \text{and} \quad \mathbf{U}_A \Psi = \begin{pmatrix} e^{i\frac{1}{2}\gamma_5 \tau^A \beta^A} & 0 \\ 0 & e^{i\frac{1}{2}\gamma_5 \tau^{A*} \beta^A} \end{pmatrix} \Psi. \quad (\text{A52})$$

The vector and axial-vector currents are diagonal in the Nambu-Gorkov formalism, since they result as Noether currents from the diagonal kinetic term

$$\bar{\Psi} i\gamma^\mu \partial_\mu \rho_0 \Psi = \begin{pmatrix} \bar{\psi} \gamma^\mu \partial_\mu \psi & 0 \\ 0 & \psi^T \gamma^{\mu T} \partial_\mu \bar{\psi}^T \end{pmatrix} = \bar{\Psi} \begin{pmatrix} \gamma^\mu \partial_\mu & 0 \\ 0 & -C \gamma^{\mu T} C^{-1} \partial_\mu \end{pmatrix} \Psi,$$

with ρ_0 the unit matrix in the Nambu-Gorkov space. Alternatively, they can be derived by a prescription from [10] which generalizes the standard current structure $\bar{\psi} \Gamma \psi$ to the charge conjugated sector as $\bar{\psi}_C C \Gamma^T C^{-1} \psi_C$. Because of $\gamma_\mu^T = -C^{-1} \gamma_\mu C$ and $C^{-1} \gamma_5 C = \gamma_5^T = \gamma_5$, we have

$$\begin{aligned} \mathbf{V}_\mu^A &\equiv \bar{\Psi} \begin{pmatrix} \gamma_\mu \frac{1}{2} \tau^A & 0 \\ 0 & C (\gamma_\mu \frac{1}{2} \tau^A)^T C^{-1} \end{pmatrix} \Psi = \bar{\Psi} \begin{pmatrix} \gamma_\mu \frac{1}{2} \tau^A & 0 \\ 0 & -\gamma_\mu \frac{1}{2} \tau^{A*} \end{pmatrix} \Psi \\ &= \bar{\Psi} \gamma_\mu \frac{1}{2} \mathbf{T}^A \rho_3 \Psi, \end{aligned} \quad (\text{A53})$$

and

$$\begin{aligned} \mathbf{A}_\mu^a &\equiv \bar{\Psi} \begin{pmatrix} \gamma_\mu \gamma_5 \frac{1}{2} \tau^A & 0 \\ 0 & C (\gamma_\mu \gamma_5 \frac{1}{2} \tau^A)^T C^{-1} \end{pmatrix} \Psi = \bar{\Psi} \begin{pmatrix} \gamma_\mu \gamma_5 \frac{1}{2} \tau^A & 0 \\ 0 & \gamma_\mu \gamma_5 \frac{1}{2} \tau^{A*} \end{pmatrix} \Psi \\ &= \bar{\Psi} \gamma_\mu \gamma_5 \frac{1}{2} \mathbf{T}^A \Psi, \end{aligned} \quad (\text{A54})$$

with $\mathbf{T}^A = \text{diag}(\tau^A, \tau^{A*})$ and $\boldsymbol{\rho}_3$ the standard Pauli matrix. In (A54) it was used that $C\gamma_5^T\gamma_\mu^TC^{-1} = CC^{-1}\gamma_5C(-C^{-1}\gamma_\mu C)C^{-1} = -\gamma_5\gamma_\mu = \gamma_\mu\gamma_5$. Furthermore, note that the derivation of the gluon-vertex (10) is totally analogous to (A53).

7. The structure of the vertices for the generalized mesons:

Because of the particle-particle (or hole-hole) substructure, all generalized mesons have the vertex structure

$$\bar{\Psi}\Gamma_M\Psi = \bar{\Psi}\begin{pmatrix} 0 & (\Gamma_M)_{12} \\ (\Gamma_M)_{21} & 0 \end{pmatrix}\Psi. \quad (\text{A55})$$

By conjugating the 21-component $\bar{\psi}_C(\Gamma_M)_{21}\psi = \psi^TC(\Gamma_M)_{21}\psi$, namely ^{#16}

$$-\psi^\dagger\{(\Gamma_M)_{21}\}^\dagger C^\dagger\psi^{T\dagger} = -\bar{\psi}\gamma^0\{(\Gamma_M)_{21}\}^\dagger\gamma^0\gamma^0C^{-1}\psi^{\dagger T} = \bar{\psi}\gamma^0\{(\Gamma_M)_{21}\}^\dagger\gamma^0C(\bar{\psi})^T, \quad (\text{A56})$$

one can derive a general rule (see [10]) which links the 12 and 21 components of Γ_M

$$(\Gamma_M)_{12} = \gamma^0\{(\Gamma_M)_{21}\}^\dagger\gamma^0. \quad (\text{A57})$$

Thus, in order to determine the structure of the generalized vertices, we only have to determine the structure of the 21-component.

As in the standard case, the structure of the (generalized) meson vertices follows from the transformation properties of the (hermitean) bilinears $\bar{\Psi}\Gamma_M\Psi$ under proper (ordinary continuous) Lorentz transformations $\psi(x) \rightarrow \psi'(x') = S(\Lambda)\psi(\Lambda x)$ with $S(\Lambda) = \exp(-\frac{i}{4}\sigma_{\alpha\beta}\omega^{\alpha\beta})$ and under the (discrete) parity transformation $\psi(x) \rightarrow \psi'(x') = \gamma_0\psi(t, -\mathbf{x})$. Using that $S(\Lambda)^T = CS(\Lambda)^{-1}C^{-1}$ and $\gamma^{0T}C = \gamma^0C = -C\gamma^0$, we can easily derive the following transformation properties of the bilinears $\bar{\psi}_C(\Gamma_M)_{21}\psi$ under proper Lorentz and parity transformations (which generalize the transformation properties of the standard bilinears $\bar{\psi}\Gamma\psi$, see e.g. [25]):

$$\begin{aligned} \bar{\psi}'_C(x')\gamma_5\psi'(x') &= \bar{\psi}_C(x)\gamma_5\psi(x) & \text{scalar} & \quad 0^+, \\ \bar{\psi}'_C(x')\psi'(x') &= \det(\Lambda)\bar{\psi}_C(x)\psi(x) & \text{pseudoscalar} & \quad 0^-, \\ \bar{\psi}'_C(x')\gamma^\mu\gamma_5\psi'(x') &= \Lambda^\mu_\nu\bar{\psi}_C(x)\gamma^\nu\gamma_5\psi(x) & \text{vector} & \quad 1^-, \\ \bar{\psi}'_C(x')\gamma_\mu\psi'(x') &= \det(\Lambda)\Lambda^\mu_\nu\bar{\psi}_C(x)\gamma^\nu\psi(x) & \text{axial-vector} & \quad 1^+. \end{aligned} \quad (\text{A58})$$

Note the appearance of the extra γ_5 relative to the standard rules of e.g. [25]. Taking the flavor matrix in the color-flavor-locked way into account, we have the following 21

^{#16}The minus sign results from the Grassman property of the fermion spinors. Note that $C = -C^\dagger = -C^{-1}$ and $\gamma_0C^{-1} = -C\gamma^{0T}$.

components of the generalized meson vertices:

$$\begin{aligned}
(\Gamma_\sigma(p, P))_{21} &= i\mathbf{M}^A \Gamma_S(p, P)/F_S && \text{generalized sigma ,} \\
(\Gamma_\pi(p, P))_{21} &= i\gamma_5 \mathbf{M}^A \Gamma_{PS}(p, P)/F_{PS} && \text{generalized pion ,} \\
(\Gamma_\mu(p, P))_{21} &= \gamma_\mu \mathbf{M}^A \Gamma_V(p, P)/F_V && \text{generalized vector meson ,} \\
(\Gamma_{5\mu}(p, P))_{21} &= i\gamma_\mu \gamma_5 \mathbf{M}^A \Gamma_{AV}(p, P)/F_{AV} && \text{generalized axial-vector meson ,}
\end{aligned} \tag{A59}$$

where $\mathbf{M}^A \equiv \gamma_5 \epsilon_f^a \epsilon_c^\alpha (\tau^A)^{a\alpha}$ and $(\epsilon^a)^{bc} = \epsilon^{abc}$. The form factors and decay constants have been introduced in [9] for the pionic case and in (43) for the vector case. Note that after inserting unity $\mathbf{1} = \Lambda^+(\mathbf{p}) + \Lambda^-(\mathbf{p})$ to the left and right of the $(\Gamma_M(p, P))_{21}$'s, we can project these vertices onto the particle-particle, particle-antiparticle, antiparticle-particle and antiparticle-antiparticle sectors in analogy to (A3):

$$\begin{aligned}
(\Gamma_M(p, P))_{21} &= \Lambda^+(\mathbf{p}) (\Gamma_M(p, P))_{pp} \Lambda^+(\mathbf{p}) + \Lambda^+(\mathbf{p}) (\Gamma_M(p, P))_{pa} \Lambda^-(\mathbf{p}) \\
&\quad + \Lambda^-(\mathbf{p}) (\Gamma_M(p, P))_{ap} \Lambda^+(\mathbf{p}) + \Lambda^-(\mathbf{p}) (\Gamma_M(p, P))_{aa} \Lambda^-(\mathbf{p}) .
\end{aligned} \tag{A60}$$

In the scalar and pseudoscalar case, the mixed (particle-antiparticle and antiparticle-particle) vertices vanish identically since $\Lambda^\pm(\mathbf{p}) \gamma_5 \Lambda^\mp(\mathbf{p}) = 0 = \Lambda^\pm(\mathbf{p}) \Lambda^\mp(\mathbf{p})$. The sum of the remaining particle-particle and antiparticle-antiparticle has exactly the structure of (A3). In the vector and axialvector case, the mixed terms $(\Gamma_M(p, P))_{pa}$ and $(\Gamma_M(p, P))_{ap}$ survive. However, in the leading-logarithm approximation only the particle-particle parts $(\Gamma_M(p, P))_{pp}$ of the vertices are needed.

Contrary to the standard case, the phases cannot be determined from the hermiticity property of the quark bilinears, since the hermiticity is automatically satisfied under the condition (A57). In general, the form factors are complex-valued, such that the phases can be chosen at will. Our phase choice corresponds to real-valued form factors with attractive Bethe-Salpeter kernels (see (42) and (A66)). Taking the (A57) rule into account, we have

$$\begin{aligned}
\Gamma_\sigma^A(p, P) &= i\boldsymbol{\rho}_1 \mathbf{M}_{\mathbf{T}}^A \Gamma_S(p, P)/F_S && \text{generalized sigma ,} \\
\Gamma_\pi^A(p, P) &= \gamma_5 \boldsymbol{\rho}_2 \mathbf{M}_{\mathbf{T}}^A \Gamma_{PS}(p, P)/F_{PS} && \text{generalized pion ,} \\
\Gamma_\mu^A(p, P) &= \gamma_\mu \boldsymbol{\rho}_1 \mathbf{M}_{\mathbf{T}}^A \Gamma_V(p, P)/F_V && \text{generalized vector meson ,} \\
\Gamma_{5\mu}^A(p, P) &= \gamma_\mu \gamma_5 \boldsymbol{\rho}_2 \mathbf{M}_{\mathbf{T}}^A \Gamma_{AV}(p, P)/F_{AV} && \text{generalized axial-vector meson ,}
\end{aligned} \tag{A61}$$

where

$$\mathbf{M}_{\mathbf{T}}^A \equiv \begin{pmatrix} \mathbf{M}^A & 0 \\ 0 & \mathbf{M}^{A\dagger} \end{pmatrix} = \begin{pmatrix} \mathbf{M}^{i\alpha} (\tau^A)^{i\alpha} & 0 \\ 0 & \mathbf{M}^{i\alpha} (\tau^{A*})^{i\alpha} \end{pmatrix} = \mathbf{M}^{i\alpha} (\mathbf{T}^A)^{i\alpha} \tag{A62}$$

and $\boldsymbol{\rho}_1$ and $\boldsymbol{\rho}_2$ are the standard Pauli matrices acting on the Nambu-Gorkov indices. As mentioned above, the form factors $\Gamma_S(p, P)$, $\Gamma_{PS}(p, P)$, $\Gamma_V(p, P)$ and $\Gamma_{AV}(p, P)$ are now assumed to be real, where $\Gamma_{PS}(p, 0) = G(p)$. The vertex structure of (A61) is in agreement with (11) and (12) as well as (43) as used in (38).

If $(\Gamma_M(p, P))_{21}$ is projected onto the particle-particle, particle-antiparticle, antiparticle-particle and antiparticle-antiparticle sectors as in (A60), it follows from the (A57)-rule and $\gamma^0 \Lambda^\pm(\mathbf{p}) \gamma^0 = \Lambda^\mp(\mathbf{p})$ that the corresponding contributions of the 1-2 component read

$$\begin{aligned} (\Gamma_M(p, P))_{12} = & \Lambda^-(\mathbf{p}) \gamma^0 (\Gamma_M(p, P))_{pp}^\dagger \gamma^0 \Lambda^-(\mathbf{p}) + \Lambda^-(\mathbf{p}) \gamma^0 (\Gamma_M(p, P))_{pa}^\dagger \gamma^0 \Lambda^+(\mathbf{p}) \\ & + \Lambda^+(\mathbf{p}) \gamma^0 (\Gamma_M(p, P))_{ap}^\dagger \gamma^0 \Lambda^-(\mathbf{p}) + \Lambda^+(\mathbf{p}) \gamma^0 (\Gamma_M(p, P))_{aa}^\dagger \gamma^0 \Lambda^+(\mathbf{p}) \end{aligned} \quad (\text{A63})$$

in analogy to (A4). In the leading logarithm approximation, only the first term, i.e. the particle-particle term, is needed. In this case the vertex structure (A61) has to be modified by the “sandwich-rule” (28) which is compatible with (A60) and (A63). As mentioned in section 3 (see also Appendix-12), the simplified vertex structure (A61) can be used, if only *leading* propagators (1) ^{#17} are coupled to the vertex and if the simplified form (5) of the gluon propagator is used.

8. Derivation of equation (13) from (9) and equation (44) from (42):

Defining $Q \equiv q + P/2$ and $K \equiv q - P/2$, the 12 component of (42) reads:

$$\begin{aligned} (\Gamma_j^A(p, P))_{12} = & g^2 \int \frac{d^4 q}{(2\pi)^4} i\mathcal{D}(p-q) \gamma_\mu \frac{\lambda^a}{2} \left[S_{11}(Q) (\Gamma_j^A(q, P))_{12} S_{22}(K) \right. \\ & \left. + S_{12}(Q) (\Gamma_j^A(q, P))_{21} S_{12}(K) \right] (-\gamma^\mu) \frac{\lambda^{aT}}{2}. \end{aligned} \quad (\text{A64})$$

The expression for $(\Gamma_j^A(p, P))_{21}$ follows from (A64) with the replacements $1 \leftrightarrow 2$ and $\lambda^a \leftrightarrow \lambda^{aT}$. We now write $(\Gamma_j^A)_{12} = \frac{1}{F_V} \gamma_j \Gamma_V \mathbf{M}^{A\dagger}$ where we assumed Γ_V to be real. Inserting then (1) for the propagators, we can transform (A64) to ^{#18}

$$\begin{aligned} \gamma_j \Gamma_V(p, P) \mathbf{M}^{A\dagger} = & -g^2 \int \frac{d^4 q}{(2\pi)^4} \frac{i\mathcal{D}(p-q) \Gamma_V(q, P)}{(Q_0^2 - \epsilon_Q^2)(K_0^2 - \epsilon_K^2)} \\ & \times \left\{ Q_+ K_- \left[\gamma_\mu \gamma^0 \Lambda^-(\mathbf{Q}) \gamma_j \gamma^0 \Lambda^+(\mathbf{K}) \gamma^\mu \right] \left[\frac{\lambda^a}{2} \mathbf{M}^{A\dagger} \frac{\lambda^{aT}}{2} \right] \right. \\ & \left. + G(Q) G(K) \gamma_\mu \Lambda^+(\mathbf{Q}) \gamma_j \Lambda^+(\mathbf{K}) \gamma^\mu \left[\frac{\lambda^a}{2} \mathbf{M} \mathbf{M}^A \mathbf{M} \frac{\lambda^{aT}}{2} \right] \right\}, \end{aligned} \quad (\text{A65})$$

where it was used that both \mathbf{M} ($=\mathbf{M}^\dagger$) and \mathbf{M}^A contain a γ_5 matrix. Note that the corresponding expression for the composite axial-vector meson differs from (A65) by the replacement $\mathbf{M}^A \rightarrow i\gamma_5 \mathbf{M}^A$ and by an additional minus sign in front of the second term

^{#17}In the scalar and pseudoscalar case, it already is sufficient that only *one* leading propagator is coupled per vertex.

^{#18}In the following, we will use the simplified form (A61) of the generalized-meson vertex. The results for the sandwiched form (28) will be discussed at the end of this section.

on the right hand side. Using (14) for the flavor contractions and moving the γ^0 matrices through, we finally get

$$\begin{aligned} \gamma_j \Gamma_V(p, P) = & -\frac{2g^2}{3} \int \frac{d^4 q}{(2\pi)^4} \frac{i\mathcal{D}(p-q) \Gamma_V(q, P)}{(Q_0^2 - \epsilon_Q^2)(K_0^2 - \epsilon_K^2)} \\ & \times \{Q_+ K_- - G(Q)G(K)\} [\gamma_\mu \Lambda^+(\mathbf{Q}) \gamma_j \Lambda^+(\mathbf{K}) \gamma^\mu] , \end{aligned} \quad (\text{A66})$$

where we ignored a symmetric contribution in color-flavor which is subleading to logarithmic accuracy. This equation will be simplified by applying the longitudinal and transverse projection (39) and (40), respectively, and then taking the Dirac trace. The left hand side becomes $4\Gamma_{L,T}(p, P)$, whereas on the right hand side the Dirac structure becomes

$$\begin{aligned} \frac{1}{3} \text{Tr} [\gamma^j \gamma_\mu \Lambda^+(\mathbf{Q}) \gamma_j \Lambda^+(\mathbf{K}) \gamma^\mu] &= -\frac{2}{3} \text{Tr} [\gamma^j \Lambda^+(\mathbf{Q}) \gamma_j \Lambda^+(\mathbf{K})] \\ &= -\frac{2}{3} \text{Tr} [(3\Lambda^+(\mathbf{Q}) - \hat{\mathbf{Q}}^k \alpha^k) \Lambda^+(\mathbf{K})] , \end{aligned} \quad (\text{A67})$$

where we summed over the index j and used the Dirac matrix identity $\gamma_\mu \gamma_j \gamma^\mu = -2\gamma_j$. In the rest frame, the trace (A67) is just $-8/3$. Inserting this back into (A66) and dividing by four, we get the quoted result (44) which identically holds in the axial-vector case.

For deriving the corresponding expression of the generalized pion from (9), the γ_j matrices in (A65) and (A66) have to be replaced by $-i\gamma_5$. After multiplying both sides with $i\gamma_5$ and then taking the Dirac trace, we still get $4\Gamma_{PS}(p, P)$ on the left hand side, whereas on the right hand the Dirac trace

$$\text{Tr} [\gamma_5 \gamma_\mu \Lambda^+(\mathbf{Q}) \gamma_5 \Lambda^+(\mathbf{K}) \gamma^\mu] = -\text{Tr} [\gamma^\mu \gamma_\mu \Lambda^+(\mathbf{Q}) \Lambda^+(\mathbf{K})] = -4\text{Tr} [\Lambda^+(\mathbf{Q}) \Lambda^+(\mathbf{K})]$$

reduces to a factor -8 instead of $-8/3$ in the rest frame. This is the reason why the prefactor in the Bethe-Salpeter kernel of the generalized pion (see (13) or (4) for the gap itself) is three times bigger than the one of the generalized vector and axial-vector (see (44)).

For the generalized sigma, the γ_j in (A65) and (A66) has to be replaced by the i times the unit matrix. Furthermore, there is an additional minus sign in front of the second term on the right hand side of (A65) and an additional overall minus sign on the right hand side of (A66). After multiplying both sides with $-i$ and taking the Dirac trace, there is still $4\Gamma_S(p, P)$ on the left hand side, whereas on the right hand side the Dirac trace

$$\text{Tr} [\gamma_\mu \Lambda^+(\mathbf{Q}) \Lambda^+(\mathbf{K}) \gamma^\mu] = 4\text{Tr} [\Lambda^+(\mathbf{Q}) \Lambda^+(\mathbf{K})]$$

reduces to $+8$ in the rest frame. This opposite sign, relative to the pion case, cancels against the above mentioned opposite sign on the right hand side of (A66). Thus the Bethe-Salpeter equation of the generalized sigma and pion are the same, see (13).

If the sandwiched form of the generalized mesons is used, equation (A66) must be first projected from the left and right with $\Lambda^-(p)$, before we can multiply with γ_j (or correspondingly with $-i\gamma_5$ in the pion or $i\mathbf{1}$ in the scalar case) and take the Dirac trace. This modification induces a factor $\frac{1}{2}$ on the left *and* right hand side of the projected (A66)

and therefore does not change the final answer (44) and (13) for the gap equations for the (axial-)vector and (pseudo-)scalar case, respectively.

The result of (A66) is valid for the phase choice of (A59), i.e. for real-valued form factors. If the opposite phase-choice had been made, i.e. if the form factors were assumed to be purely imaginary-valued, the $Q_+K_- - G(Q)G(K)$ term in (A66) would have to read $Q_+K_- + G(Q)G(K)$ instead. The error which this choice will induce can be estimated by perturbation theory by inserting (6) and (49) or an analogous form factor into

$$\frac{h_*^2}{18} \int_{G_M}^{\Lambda_*} \frac{dq_{||}}{q_{||}} \frac{-2G^2(q_{||})}{q_{||}^2} \ln \left(\frac{\Lambda_*^2}{(p_{||} - q_{||})^2} \right) \Gamma(q_{||}, M_V) \quad (\text{A68})$$

as very small, i.e. $\mathcal{O}(h_*^2)$ relatively to $\Gamma(q_{||}, M_V)$.

9. The structure of the vertices for the standard mesons:

The Bethe-Salpeter kernels of the diagonal *standard* “ $\bar{q} q$ ” -type mesons in the CFL phase are

$$\begin{aligned} \tilde{\Gamma}_\sigma^A(p, P) &= \boldsymbol{\rho}_0 \mathbf{N}_{\tilde{T}}^A \tilde{\Gamma}_S(p, P) / \tilde{F}_\Sigma && \text{standard sigma ,} \\ \tilde{\Gamma}_\pi^A(p, P) &= i\gamma_5 \boldsymbol{\rho}_0 \mathbf{N}_{\tilde{T}}^A \tilde{\Gamma}_{PS}(p, P) / \tilde{F} && \text{standard pion ,} \\ \tilde{\Gamma}_\mu^A(p, P) &= \gamma_\mu \boldsymbol{\rho}_3 \mathbf{N}_{\tilde{T}}^A \tilde{\Gamma}_V(p, P) / \tilde{F}_V && \text{standard vector meson ,} \\ \tilde{\Gamma}_{5\mu}^A(p, P) &= \gamma_\mu \gamma_5 \boldsymbol{\rho}_0 \mathbf{N}_{\tilde{T}}^A \tilde{\Gamma}_{AV}(p, P) / \tilde{F}_{AV} && \text{standard axial-vector meson ,} \end{aligned} \quad (\text{A69})$$

where $\mathbf{N}_{\tilde{T}}^A = \epsilon_f^a \epsilon_c^\alpha (\tilde{T}^A)^{a\alpha}$. Thus $\mathbf{N}_{\tilde{T}}^A$ is of the same form as $\mathbf{M}_{\mathbf{T}}^A$, without the γ_5 , however, and with $\mathbf{T}^A = \text{diag}(\tau^A, \tau^{A*})$ replaced by $\tilde{T}^A = \text{diag}(\tilde{\tau}^A, \tilde{\tau}^A)$, where $\tilde{\tau}_{1,3} = \tau_{1,3}$ and $\tilde{\tau}_2 = i\tau_2$. Furthermore $\boldsymbol{\rho}_3$ is the usual Pauli matrix, whereas $\boldsymbol{\rho}_0$ is the corresponding unit matrix. We have checked that the Bethe-Salpeter equations resulting from (A69) vanish identically. Standard scalar, pseudoscalar, vector and axial-vector excitations are not supported by the QCD superconductor in leading logarithm approximation.

10. From equation (15) to equation (20) and other variational approximations:

After multiplying (15) with $3/4g^2$ and using the Fourier-transformations

$$\begin{aligned} \Gamma(p, M) &= \int d^4x e^{ipx} \Gamma(x) , \\ \mathcal{D}(p - q) &= \int d^4x e^{i(p-q)x} \mathcal{D}(x) , \end{aligned}$$

we can transform (15) into

$$\frac{3}{4g^2} \Gamma(x) = \int \frac{d^4q}{(2\pi)^4} e^{-iqx} i\mathcal{D}(x) \frac{q_0^2 - \epsilon_q^2 - M^2/4}{(q_0^2 - \epsilon_q^2 + M^2/4)^2 - M^2 q_0^2} \Gamma(q) ,$$

where $\Gamma(q) \equiv \Gamma(q, M)$. Multiplying both sides with $\Gamma(x)/i\mathcal{D}(x)$ and integrating over x , we get

$$\begin{aligned} \frac{3}{4g^2} \int d^4x \frac{\Gamma^2(x)}{i\mathcal{D}(x)} &= \int \frac{d^4q}{(2\pi)^4} \left\{ \int d^4x e^{-iqx} \Gamma(x) \right\} \frac{q_0^2 - \epsilon_q^2 - M^2/4}{(q_0^2 - \epsilon_q^2 + M^2/4)^2 - M^2 q_0^2} \Gamma(q) \\ &= \int \frac{d^4q}{(2\pi)^4} \Gamma(-q) \frac{q_0^2 - \epsilon_q^2 - M^2/4}{(q_0^2 - \epsilon_q^2 + M^2/4)^2 - M^2 q_0^2} \Gamma(q) . \end{aligned}$$

Assuming that $\Gamma(q)$ is an even function in q in analogy to $G(q)$ and Taylor-expanding the right-hand side in M^2 , we get (17), i.e.

$$\begin{aligned} \frac{3}{4g^2} \int d^4x \frac{\Gamma^2(x)}{i\mathcal{D}(x)} &\approx \int \frac{d^4q}{(2\pi)^4} \frac{\Gamma^2(q)}{q_0^2 - \epsilon_q^2} + \frac{M^2}{4} \int \frac{d^4q}{(2\pi)^4} \frac{q_0^2 + 3\epsilon_q^2}{(q_0^2 - \epsilon_q^2)^3} \Gamma^2(q) \\ &= \int \frac{d^4q}{(2\pi)^4} \frac{\Gamma^2(q)}{q_0^2 - \epsilon_q^2} - iM^2 F^2 , \end{aligned}$$

where definition (18) was used. By assuming that $\Gamma(q) = \kappa G(q)$ is an even real-valued function of $q_{||}$, by Wick-rotating to Euclidean space and evaluating the resulting q_4 integration as a contour integration, we can calculate F^2 defined in the last equation as follows:

$$\begin{aligned} F^2 &\equiv \frac{i}{4} \int \frac{d^4q}{(2\pi)^4} \frac{q_0^2 + 3\epsilon_q^2}{(q_0^2 - \epsilon_q^2)^3} \Gamma^2(q) \\ &= \frac{1}{4} 2\pi \int_0^{2\mu} \frac{q_{\perp} dq_{\perp}}{(2\pi)^2} 2 \int_0^{\infty} \frac{dq_{||}}{2\pi} \Gamma^2(q_{||}) \int_{-\infty}^{+\infty} \frac{dq_4}{2\pi} \frac{-q_4^2 + \epsilon_q^2}{(q_4 - i\epsilon_q)^3 (q_4 + i\epsilon_q)^3} \\ &= \frac{1}{4} \frac{\mu^2}{\pi^2} \int_0^{\infty} dq_{||} \Gamma^2(q_{||}) \frac{2\pi i}{2\pi} \frac{1}{i2\epsilon_q^3} \\ &= \frac{\mu^2}{8\pi^2} \int_0^{\infty} dq_{||} \frac{\Gamma^2(q_{||})}{\epsilon_q^3} = \frac{\kappa^2 \mu^2}{8\pi^2} \int_0^{\infty} dq_{||} \frac{G^2(q_{||})}{\epsilon_q^3} \approx \frac{\kappa^2 \mu^2}{8\pi^2} \int_{G_0}^{\Lambda_*} dq_{||} \frac{G^2(q_{||})}{q_{||}^3} . \end{aligned}$$

After inserting (6) into the last equation and shifting to the logarithmic scales $x = \ln(\Lambda_*/q_{||})$ and $x_0 = \ln(\Lambda_*/G_0)$, one finally arrives at (20), i.e.

$$F^2 \approx \frac{\kappa^2 \mu^2}{8\pi^2} \int_0^{x_0} dx e^{2(x-x_0)} \sin^2(\pi x/2x_0) = \frac{\kappa^2 \mu^2}{8\pi^2} \frac{8x_0^2 + \pi^2 - e^{-2x_0}\pi^2}{16x_0^2 + 4\pi^2} \approx \frac{\kappa^2 \mu^2}{16\pi^2} , \quad (\text{A70})$$

since $x_0 \gg 1$, see [9].

Finally note the variational approximation

$$\begin{aligned} \int \frac{d^4q}{(2\pi)^4} \frac{\Gamma_{T,L}^2(q)}{q_0^2 - \epsilon_q^2} &= 2\pi \int_0^{2\mu} \frac{q_{\perp} dq_{\perp}}{(2\pi)^2} 2 \int_0^{\infty} \frac{dq_{||}}{2\pi} \Gamma_{T,L}^2(q_{||}) \int \frac{idq_4}{2\pi} \frac{1}{-q_4^2 - \epsilon_q^2} \\ &= -i \frac{\mu^2}{\pi^2} \int_0^{\infty} dq_{||} \frac{\Gamma_{T,L}^2(q_{||})}{2\epsilon_q} \\ &\approx -i \frac{\kappa^2 \mu^2}{2\pi^2} \int_{G_0}^{\Lambda_*} dq_{||} \frac{G_M^2 \sin^2\left(\frac{h_*}{3} \ln\left(\frac{\Lambda_*}{q_{||}}\right)\right)}{q_{||}} \\ &= -i \frac{\kappa^2 \mu^2 G_M^2}{2\pi^2} \int_0^{x_0} dx \sin^2\left(\frac{\pi x}{2x_M}\right) \\ &= -i \frac{\kappa^2 \mu^2 G_M^2}{4\pi^2} x_0 \left(1 - \frac{x_M}{\pi x_0} \sin\left(\frac{\pi x_0}{x_M}\right)\right) , \end{aligned}$$

which is used to derive (57) from the vector-meson analog of (17).

11. Gluon polarization function in the CFL phase:

In the CFL phase, the gluon polarization function for the bare gluon (AA) fields is

$$\Pi_{\mu\nu}^{ab}(Q) = -g^2 \int \frac{d^4 q}{(2\pi)^4} \text{Tr} \left(i\mathcal{V}_\mu^a i\mathbf{S}(q + \frac{Q}{2}) i\mathcal{V}_\nu^b i\mathbf{S}(q - \frac{Q}{2}) \right). \quad (\text{A71})$$

Using $\text{Tr}_{cf}(\lambda^a \lambda^b) = 6 \delta^{ab}$ and

$$\text{Tr}_{cf}(\lambda^a \mathbf{M} \lambda^{bT} \mathbf{M}) = -2 \text{Tr}_c(\lambda^a \lambda^b) = -4 \delta^{ab},$$

we may write (A71) in the following form

$$\begin{aligned} \Pi_{\mu\nu}^{ab}(Q) = & -g^2 \delta^{ab} \int \frac{d^4 q}{(2\pi)^4} \frac{1}{(K_0^2 - \epsilon_K^2)(P_0^2 - \epsilon_P^2)} \\ & \times \left\{ 3 \left(K_0 P_0 + K_{||} P_{||} \right) \text{Tr} \left[\gamma_\mu \gamma^0 \Lambda^-(K) \gamma_\nu \gamma^0 \Lambda^-(P) \right] \right. \\ & \left. + 2G(K)G(P) \text{Tr} \left[\gamma_\mu \Lambda^+(K) \gamma_\nu \Lambda^-(P) \right] \right\} \end{aligned} \quad (\text{A72})$$

with $K = q + Q/2$ and $P = q - Q/2$.

For the temporal polarization, we have

$$\Pi_{00}^{ab}(Q) = -g^2 \delta^{ab} \int \frac{d^4 q}{(2\pi)^4} \frac{3(K_0 P_0 + K_{||} P_{||}) + 2G(K)G(P)}{(K_0^2 - \epsilon_K^2)(P_0^2 - \epsilon_P^2)} (1 + \hat{K} \cdot \hat{P}). \quad (\text{A73})$$

For $Q = 0$, this simplifies to

$$\begin{aligned} \Pi_{00}^{ab}(0) = & -g^2 \delta^{ab} \int \frac{d^4 q}{(2\pi)^4} \frac{6(q_0^2 + q_{||}^2) + 4G^2(q)}{(q_0^2 - \epsilon_q^2)^2} \\ = & -\delta^{ab} \frac{g^2 \mu^2}{\pi^2} \int_0^\infty dq_{||} \int_{-\infty}^{+\infty} \frac{dq_4}{2\pi} \frac{-6q_4^2 + 6\epsilon_q^2 - 2G^2(q)}{(q_4^2 + \epsilon_q^2)^2} \\ = & \delta^{ab} \frac{g^2 \mu^2}{\pi^2} \int_0^\infty dq_{||} \frac{iG^2(q)}{2\epsilon_q^3} = i\delta^{ab} \left(\frac{g\mu}{2\pi} \right)^2. \end{aligned} \quad (\text{A74})$$

Here we have used that the angle and q_\perp integrations contribute a factor $2\pi 2\mu^2$ and, after a Wick rotation to Euclidean space and contour integration, that $\int_0^\infty dq_{||} G^2(q)/\epsilon_q^3 = 1/2$ (see above).

For the spatial polarization, we obtain

$$\Pi_{ij}^{ab}(Q) = g^2 \delta^{ab} \int \frac{d^4 q}{(2\pi)^4} \frac{3(K_0 P_0 + K_{||} P_{||}) - 2G(K)G(P)}{(K_0^2 - \epsilon_K^2)(P_0^2 - \epsilon_P^2)} (g_{ij}(1 - \hat{K} \cdot \hat{P}) - \hat{K}_i \hat{P}_j - \hat{K}_j \hat{P}_i) \quad (\text{A75})$$

after using the spin trace

$$\text{Tr} [\gamma^i \Lambda^\pm(\mathbf{K}) \gamma^j \Lambda^\mp(\mathbf{P})] = g^{ij} - (g^{im} g^{jn} - g^{ij} g^{mn} + g^{in} g^{jm}) \hat{\mathbf{K}}^m \hat{\mathbf{P}}^n. \quad (\text{A76})$$

For $Q = 0$, this simplifies

$$\begin{aligned}
\Pi_{ij}^{ab}(0) &= -g^2 \delta^{ab} \int \frac{d^4 q}{(2\pi)^4} \frac{6(q_0^2 + q_{||}^2) - 4G^2(q)}{(q_0^2 - \epsilon_q^2)^2} \hat{\mathbf{q}}_i \hat{\mathbf{q}}_j \\
&= -\frac{1}{3} g^2 \delta^{ab} \delta_{ij} \int \frac{d^4 q}{(2\pi)^4} \frac{6q_0^2 + 6\epsilon_q^2 - 10G^2(q)}{(q_0^2 - \epsilon_q^2)^2} \\
&= \frac{5}{6} \delta^{ab} \delta_{ij} \frac{g^2 \mu^2}{\pi^2} \int_0^\infty dq_{||} \frac{iG^2(q)}{\epsilon_q^3} = i \delta^{ab} \delta_{ij} \frac{5g^2 \mu^2}{12\pi^2} .
\end{aligned} \tag{A77}$$

The lack of transversality in the AA polarization, which is manifest in (A74) and (A77), is fixed by the mixing with the scalars (Higgs mechanism) and the additional contribution from the modes within the Fermi surface (nonsurface modes).

12. The comparison of the exact and simplified in-medium gluon propagator:

According to eq. (6.51) of [13] and eq. (10) of [15], the in-medium retarded (Minkowski-space) gluon-propagator in a general covariant gauge reads (modulo an overall phase factor)

$$\mathcal{D}_{\mu\nu}(q) = i \frac{P_{\mu\nu}^T}{q^2 - G} + i \frac{P_{\mu\nu}^L}{q^2 - F} - i \xi \frac{P_{\mu\nu}^{GF}}{q^2} , \tag{A78}$$

where $F \equiv m_D^2 = \frac{N_f}{2\pi^2} g^2 \mu^2$ ($\equiv m_E^2$) and $G = \frac{\pi}{4} \frac{-iq_0}{|\mathbf{q}|} m_D^2$ ($\equiv m_M^2$). The propagator contains the gauge parameter ξ , which must not appear in physical results. The projectors appearing in (A78) read

$$P_{\mu\nu}^T = (1 - g_{\mu 0})(1 - g_{\nu 0}) \left(-g_{\mu\nu} - \frac{q_\mu q_\nu}{\mathbf{q}^2} \right) , \tag{A79}$$

$$P_{\mu\nu}^L = -g_{\mu\nu} + \frac{q_\mu q_\nu}{q^2} - P_{\mu\nu}^T , \tag{A80}$$

$$P_{\mu\nu}^{GF} = \frac{q_\mu q_\nu}{q^2} , \tag{A81}$$

where $q^2 = (q^0)^2 - \mathbf{q}^2$ and $g_{\mu\nu} = g^{\mu\nu} = \text{diag}(1, -1, -1, -1)$ for $\mu, \nu = 0, 1, 2, 3$. The transverse projector can be written as

$$P_{\mu 0}^T = P_{0\nu}^T = 0 , \tag{A82}$$

$$P_{ij}^T = P_{ji}^T = \delta_{ij} - \hat{\mathbf{q}}_i \hat{\mathbf{q}}_j , \tag{A83}$$

where $\hat{\mathbf{q}}_i \equiv q_i/|\mathbf{q}|$. Eq. (A78) should be compared with the simplified form

$$\mathcal{D}_{\mu\nu}(q) = i \frac{1}{2} \frac{-g_{\mu\nu}}{q^2 - G} + i \frac{1}{2} \frac{-g_{\mu\nu}}{q^2 - F} , \tag{A84}$$

which is the analog in Minkowski space of the screened perturbative gluon propagator in Euclidean space used here in (5), see also [12, 9]. We now proceed to show that (A78-A84) yield equivalent results in the context of our analysis.

The three-momentum can be split into the Fermi-momentum \mathbf{q}_F and a momentum \vec{l} measured relative to the Fermi surface,

$$|\mathbf{q}| = |\mathbf{q}_F + \vec{l}| = \mu + l_{||} + \frac{l_{\perp}^2}{2\mu} + \mathcal{O}(1/\mu^2), \quad (\text{A85})$$

where $l_{||}$ and l_{\perp} are the projections of the relative momentum in the direction of and orthogonal to the Fermi-momentum \mathbf{P} , respectively. Because of the decomposition (A85), we have, modulo $1/\mu^2$ corrections, $q^2 = q_0^2 - \mathbf{q}^2 \approx -\mathbf{q}^2$ and we can simplify the longitudinal projector as follows (see [15]))

$$P_{\mu\nu}^L \approx -g_{\mu 0} g_{\nu 0}. \quad (\text{A86})$$

Finally we will use that

$$\delta^{ij} P_{ij}^T = 2, \quad (\text{A87})$$

$$\hat{\mathbf{q}} \cdot \hat{\mathbf{Q}} \hat{\mathbf{k}} \cdot \hat{\mathbf{Q}} = -\frac{1}{2} (1 - \hat{\mathbf{q}} \cdot \hat{\mathbf{k}}) + \mathcal{O}(1/\mu), \quad (\text{A88})$$

where $Q \equiv k - q$. The second formula can be derived with the help of eq. (A85) applied to $|\mathbf{k}|$, $|\mathbf{q}|$ and $|\mathbf{Q}| = |\mathbf{k} - \mathbf{q}|$, i.e., $|\mathbf{Q}|^2 = |\mathbf{k} - \mathbf{q}|^2 \approx 2\mu^2 (1 - \hat{\mathbf{q}} \cdot \hat{\mathbf{k}})$ and $\hat{\mathbf{q}} \cdot \mathbf{Q} \hat{\mathbf{k}} \cdot \mathbf{Q} = (|\mathbf{k}| \hat{\mathbf{q}} \cdot \hat{\mathbf{k}} - |\mathbf{q}|)(|\mathbf{k}| - |\mathbf{q}| \hat{\mathbf{q}} \cdot \hat{\mathbf{k}}) \approx -\mu^2 (1 - \hat{\mathbf{q}} \cdot \hat{\mathbf{k}})^2$.

The Dirac structure of the gap equation of [15] (and of the Bethe-Salpeter equation (9) *in case* the generalized-pion-vertex follows the sandwich rule (28), i.e., the projectors $\frac{1}{2}(1 \pm \boldsymbol{\alpha} \cdot \hat{\mathbf{q}})$ are kept in the generalized-pion-vertex (12)) reads:

$$\begin{aligned} A^{\mu\nu} &\equiv \frac{1}{2} \text{Tr} \left[\gamma^\mu \frac{1}{2} (1 - s_R \gamma^0 \gamma^m \hat{\mathbf{q}}^m) \gamma^\nu \frac{1}{2} (1 + s_L \gamma^0 \gamma^n \hat{\mathbf{k}}^n) \right] \\ &= \frac{1}{2} g^{\mu\nu} + \frac{s_L}{2} (g^{\mu n} g^{\nu 0} - g^{\mu 0} g^{\nu n}) \hat{\mathbf{k}}^n + \frac{s_R}{2} (g^{\mu m} g^{\nu 0} - g^{\mu 0} g^{\nu m}) \hat{\mathbf{q}}^m \\ &\quad + \frac{s_R s_L}{2} (2g^{\mu 0} g^{\nu 0} \delta^{mn} - g^{\mu\nu} \delta^{mn} - g^{\mu m} g^{\nu n} - g^{\mu n} g^{\nu m}) \hat{\mathbf{q}}^m \hat{\mathbf{k}}^n, \end{aligned} \quad (\text{A89})$$

where $s_L = s_R = \pm 1$ for the gap and $s_L = -s_R = \pm 1$ for the anti-gap, see eq. (9) of [15].

The Dirac structure of the Bethe-Salpeter equation (9) *without* the projectors $\frac{1}{2}(1 \pm \boldsymbol{\alpha} \cdot \hat{\mathbf{q}})$ in the generalized-pion-vertex (12) reads

$$\begin{aligned} B^{\mu\nu} &= \frac{1}{4} \text{Tr} [\gamma^\mu \frac{1}{2} (1 \mp \gamma^0 \gamma^m \hat{\mathbf{q}}^m) \gamma^\nu] \\ &= \frac{1}{2} g^{\mu\nu} \mp \frac{1}{2} (g^{\mu 0} g^{\nu m} - g^{\mu m} g^{\nu 0}) \hat{\mathbf{q}}^m. \end{aligned} \quad (\text{A90})$$

Here, the projector $\frac{1}{2}(1 \mp \gamma^0 \gamma^m \hat{\mathbf{q}}^m)$ results solely from the leading parts of the quark propagators (1) and not from the generalized-pion vertex. The prefactor $\frac{1}{4}$ in (A90) versus the prefactor $\frac{1}{2}$ in (A89) can be traced back to the division by the Dirac trace on the l.h.s. of the Bethe-Salpeter equation, namely to the division by $\text{Tr}[1] = 4$ in (A90) versus $\text{Tr}[\frac{1}{2}(1 + s_L \gamma^0 \gamma^n \hat{\mathbf{k}}^n)] = 2$ in (A89).

Using the projectors of $\mathcal{D}_{\mu\nu}(k - q)$ as given in (A78), we get

$$A^{\mu\nu} P_{\mu\nu}^L = -A^{00} = -\frac{1}{2} (1 + s_R s_L \hat{\mathbf{q}} \cdot \hat{\mathbf{k}}). \quad (\text{A91})$$

Assuming as in [15] that $\hat{\mathbf{q}} \cdot \hat{\mathbf{k}} \equiv \cos(\theta) \approx 1$ in the *numerators* of the gap-equation, we get the weight -1 for the longitudinal contribution to the gap and 0 for the longitudinal contribution to the anti-gap. This should be compared with

$$B^{\mu\nu} P_{\mu\nu}^L = -\frac{1}{2} \quad (\text{A92})$$

for both the gap and the anti-gap. Note that (A92) is just the average of (A91).

Furthermore, we have using (A88)

$$\begin{aligned} A^{\mu\nu} P_{\mu\nu}^T &= \frac{1}{2} g^{ij} P_{ij}^T + \frac{s_{RSL}}{2} \left(-2P_{mn}^T + \delta^{ij} P_{ij}^T \delta^{mn} \right) \hat{\mathbf{k}}^n \hat{\mathbf{q}}^m \\ &= -1 + s_{RSL} \left(\hat{\mathbf{k}} \cdot \hat{\mathbf{q}} - \hat{\mathbf{k}} \cdot \hat{\mathbf{q}} + \hat{\mathbf{k}} \cdot \hat{\mathbf{Q}} \hat{\mathbf{q}} \cdot \hat{\mathbf{Q}} \right) \\ &\approx -1 - \frac{1}{2} s_{RSL} + \frac{1}{2} s_{RSL} \hat{\mathbf{k}} \cdot \hat{\mathbf{q}}. \end{aligned} \quad (\text{A93})$$

Under the approximation $\hat{\mathbf{k}} \cdot \hat{\mathbf{q}} \approx 1$, we get for the gap-case $-\frac{3}{2} + \frac{1}{2} \hat{\mathbf{k}} \cdot \hat{\mathbf{q}} \approx -1$ and for the anti-gap case $-\frac{1}{2} - \frac{1}{2} \hat{\mathbf{k}} \cdot \hat{\mathbf{q}} \approx -1$. This agrees with the unprojected case

$$B^{\mu\nu} P_{\mu\nu}^T = -\frac{1}{2} \delta^{ij} P_{ij}^T = -1 \quad (\text{A94})$$

for both the gap and the anti-gap.

Finally,

$$\begin{aligned} A^{\mu\nu} P_{\mu\nu}^{GF} &= \frac{1}{2} \frac{g^{\mu\nu} Q_\mu Q_\nu}{Q^2} + \frac{s_{RSL}}{2} \left(2 \frac{Q^0 Q^0}{Q^2} \hat{\mathbf{k}} \cdot \hat{\mathbf{q}} - 2 \frac{\mathbf{Q} \cdot \hat{\mathbf{k}} \mathbf{Q} \cdot \hat{\mathbf{q}}}{Q^2} - \frac{Q^2}{Q^2} \hat{\mathbf{k}} \cdot \hat{\mathbf{q}} \right) \\ &= \frac{1}{2} - \frac{s_{RSL}}{2} \hat{\mathbf{k}} \cdot \hat{\mathbf{q}} + s_{RSL} \left(\hat{\mathbf{k}} \cdot \hat{\mathbf{q}} \frac{Q^{02}}{Q^2} - \frac{\mathbf{Q} \cdot \hat{\mathbf{k}} \mathbf{Q} \cdot \hat{\mathbf{q}}}{Q^2} \right) \\ &\approx \frac{1}{2} - \frac{s_{RSL}}{2} \hat{\mathbf{k}} \cdot \hat{\mathbf{q}} + s_{RSL} \left(-\frac{\mathbf{Q} \cdot \hat{\mathbf{k}} \mathbf{Q} \cdot \hat{\mathbf{q}}}{-Q^2} \right) \\ &\approx \frac{1}{2} - \frac{s_{RSL}}{2} \hat{\mathbf{k}} \cdot \hat{\mathbf{q}} + s_{RSL} \left(\frac{1}{2} \hat{\mathbf{k}} \cdot \hat{\mathbf{q}} - \frac{1}{2} \right) \\ &= \frac{1}{2} (1 - s_{RSL}), \end{aligned} \quad (\text{A95})$$

where $Q^2 \approx -\mathbf{Q}^2$ and (A88) was used. Note that the gauge-fixing dependence vanishes for the gap and gives a weight factor $+1$ for the anti-gap.

This should be compared with

$$B^{\mu\nu} P_{\mu\nu}^{GF} = +\frac{1}{2} \quad (\text{A96})$$

for both the gap and the anti-gap. Again, the result (A96) of the unprojected case is the average of the sandwiched one, (A95).

If $A^{\mu\nu}$ is contracted with $-\frac{1}{2} g_{\mu\nu}$ as in the gluon-propagator (A84) and in the Euclidean analog (5), we get

$$\begin{aligned} A^{\mu\nu} \frac{-1}{2} g_{\mu\nu} &= -1 + \frac{s_{RSL}}{2} \left(-g^{00} \hat{\mathbf{q}} \cdot \hat{\mathbf{k}} + 2 \hat{\mathbf{q}} \cdot \hat{\mathbf{k}} + \frac{1}{2} g^{mn} \hat{\mathbf{q}}^m \hat{\mathbf{k}}^n + \frac{1}{2} g^{mn} \hat{\mathbf{q}}^m \hat{\mathbf{k}}^n \right) \\ &= -1 + \frac{s_{RSL}}{2} \left(-\hat{\mathbf{q}} \cdot \hat{\mathbf{k}} + 2 \hat{\mathbf{q}} \cdot \hat{\mathbf{k}} - \hat{\mathbf{q}} \cdot \hat{\mathbf{k}} \right) \\ &= -1 \end{aligned} \quad (\text{A97})$$

for both the gap and the anti-gap.

If $B^{\mu\nu}$ is contracted with $-\frac{1}{2}g_{\mu\nu}$, then

$$B^{\mu\nu} \frac{-1}{2} g_{\mu\nu} = -\frac{1}{4} g^{\mu\nu} g_{\mu\nu} = -1 \quad (\text{A98})$$

for both the gap and the anti-gap.

In summary: the use of the simplified propagator (5) together with the *unprojected* meson vertices, i.e. (28) without the additional projectors, yields the same results as the use of the exact propagator (A78) (or even the simplified propagator) together with the *sandwiched* meson vertices (28), to leading order. At higher order, the simplifications require amendments. To leading order, the differences resulting from (A89) and (A90) can be traced back to the presence or absence of the projector $\Lambda^\pm(\mathbf{k})$ on the l.h.s. of the Bethe-Salpeter equation, i.e. at the *amputated* vertex.

References

- [1] B.C. Barrois, Nucl. Phys. **B129**, 390 (1977); S.C. Frautschi, in *Workshop on Hadronic Matter at Extreme Energy Density*, Erice, Italy, Oct 13-21, 1978.
- [2] D. Bailin and A. Love, Phys. Lett. **107B**, 377 (1981); Phys. Rept. **107**, 325 (1984); P. Minkowski, *Extended from contribution to the Int. Symp. on Hadron Interactions, Bechyne Castle, Czechoslovakia, Jun 26 - Jul 1, 1988*; L.A. Kondratyuk, M.M. Giannini and M.I. Krivoruchenko, Phys. Lett. **B269**, 139 (1991); L.A. Kondratyuk and M.I. Krivoruchenko, Z. Phys. **A344**, 99 (1992).
- [3] M. Alford, K. Rajagopal and F. Wilczek, Phys. Lett. **B422**, 247 (1998), hep-ph/9711395; R. Rapp, T. Schäfer, E.V. Shuryak and M. Velkovsky, Phys. Rev. Lett. **81**, 53 (1998), hep-ph/9711396.
- [4] T. Schäfer, Nucl. Phys. **A638**, 511C (1998); M. Alford, K. Rajagopal and F. Wilczek, Nucl. Phys. **A638**, 515C (1998), hep-ph/9802284; K. Rajagopal, Prog. Theor. Phys. Suppl. **131**, 619 (1998), hep-ph/9803341; J. Berges and K. Rajagopal, Nucl. Phys. **B538**, 215 (1999), hep-ph/9804233; M. Alford, K. Rajagopal and F. Wilczek, Nucl. Phys. **B537**, 443 (1999), hep-ph/9804403; T. Schäfer, Nucl. Phys. **A642**, 45 (1998), nucl-th/9806064; S. Hands and S.E. Morrison [UKQCD Collaboration], Phys. Rev. **D59**, 116002 (1999), hep-lat/9807033; K. Rajagopal, Nucl. Phys. **A642**, 26 (1998), hep-ph/9807318; N. Evans, S.D.H. Hsu and M. Schwetz, Nucl. Phys. **B551**, 275 (1999), hep-ph/9808444; S. Morrison [UKQCD Collaboration], Nucl. Phys. Proc. Suppl. **73**, 480 (1999), hep-lat/9809040; M. Alford, Nucl. Phys. Proc. Suppl. **73**, 161 (1999), hep-lat/9809166. T. Schäfer and F. Wilczek, Phys. Lett. **B450**, 325 (1999), hep-ph/9810509; N. Evans, S.D.H. Hsu and M. Schwetz, Phys. Lett. **B449**, 281 (1999), hep-ph/9810514; R.D. Pisarski and D.H. Rischke, Phys. Rev. Lett. **83**, 37 (1999),

- nucl-th/9811104; K. Langfeld and M. Rho, hep-ph/9811227; J. Berges, D.U. Jungnickel and C. Wetterich, hep-ph/9811387; T. Schäfer and F. Wilczek, Phys. Rev. Lett. **82**, 3956 (1999), hep-ph/9811473; D.T. Son, Phys. Rev. **D59**, 094019 (1999), hep-ph/9812287; A. Chodos, H. Minakata and F. Cooper, Phys. Lett. **B449**, 260 (1999), hep-ph/9812305; J. Hosek, hep-ph/9812515; G.W. Carter and D. Diakonov, Phys. Rev. **D60**, 016004 (1999), hep-ph/9812445; D.K. Hong, hep-ph/9812510.
- [5] S. Hands and S. Morrison, hep-lat/9902011, hep-lat/9902012; N.O. Agasian, B.O. Kerbikov and V.I. Shevchenko, hep-ph/9902335; J. Berges, hep-ph/9902419. R.D. Pisarski and D.H. Rischke, Phys. Rev. **D60**, 094013 (1999), nucl-th/9903023; T.M. Schwarz, S.P. Klevansky and G. Papp, Phys. Rev. **C60**, 055205 (1999), nucl-th/9903048; D.G. Caldi and A. Chodos, hep-ph/9903416; M. Alford, J. Berges and K. Rajagopal, hep-ph/9903502; T. Schäfer and F. Wilczek, Phys. Rev. **D60**, 074014 (1999), hep-ph/9903503; R. Rapp, T. Schäfer, E.V. Shuryak and M. Velkovsky, hep-ph/9904353; D. Blaschke, D.M. Sedrakian and K.M. Shahabasian, astro-ph/9904395; S. Hands and S. Morrison, hep-lat/9905021; G.W. Carter and D. Diakonov, hep-ph/9905465; E. Shuster and D.T. Son, hep-ph/9905448; A. Chodos, F. Cooper and H. Minakata, hep-ph/9905521; D.K. Hong, hep-ph/9905523; R.D. Pisarski and D.H. Rischke, nucl-th/9906050; D.K. Hong, V.A. Miransky, I.A. Shovkovy and L.C. Wijewardhana, hep-ph/9906478; T. Schäfer and F. Wilczek, Phys. Rev. **D60**, 114033 (1999), hep-ph/9906512; D.K. Hong, M. Rho and I. Zahed, hep-ph/9906551; M. Rho, nucl-th/9908015; V.A. Miransky, I.A. Shovkovy and L.C. Wijewardhana, Phys. Lett. **B468**, 270 (1999), hep-ph/9908212; R. Casalbuoni and R. Gatto, Phys. Lett. **B464**, 111 (1999), hep-ph/9908227; M. Alford, J. Berges and K. Rajagopal, hep-ph/9908235; W.E. Brown, J.T. Liu and H. Ren, hep-ph/9908248; E.V. Shuryak, hep-ph/9908290; S.D.H. Hsu and M. Schwetz, hep-ph/9908310; G.W. Carter and D. Diakonov, hep-ph/9908314; D. Blaschke, T. Klahn and D.N. Voskresensky, astro-ph/9908334; F. Wilczek, hep-ph/9908480; T. Schäfer, nucl-th/9909013; A. Chodos, F. Cooper, W. Mao, H. Minakata and A. Singh, hep-ph/9909296; R. Casalbuoni and R. Gatto, hep-ph/9909419; T. Schäfer, hep-ph/9909574; I.A. Shovkovy and L.C. Wijewardhana, hep-ph/9910225; P.F. Bedaque, hep-ph/9910247; M. Alford, J. Berges and K. Rajagopal, hep-ph/9910254; B. Vanderheyden and A.D. Jackson, hep-ph/9910295; N. Evans, J. Hormuzdiar, S.D.H. Hsu, M. Schwetz, hep-ph/9910313; B.Y. Park, M. Rho, A. Wirzba and I. Zahed, hep-ph/9910347; R.D. Pisarski and D.H. Rischke, nucl-th/9910056; D.T. Son and M.A. Stephanov, hep-ph/9910491; M. Matsuzaki, hep-ph/9910541; M. Rho, A. Wirzba and I. Zahed, hep-ph/9910550; T. Schäfer, nucl-th/9911017; R. Casalbuoni and R. Gatto, hep-ph/9911223; R. D. Pisarski, nucl-th/9912070; W. E. Brown, J. T. Liu and H. Ren, hep-ph/9912409; H. Heiselberg, hep-ph/9912419; J. Madsen, astro-ph/9912418; S. Pepin, M. C. Birse, J. A. McGovern and N. R. Walet, hep-ph/9912475; S. Ying, hep-ph/9912519;

- D. K. Hong, T. Lee and D. Min, [hep-ph/9912531](#).
- [6] D.K. Hong, M. Rho and I. Zahed, Phys. Lett. **B468**, 261 (1999), [hep-ph/9906551](#).
 - [7] R. Casalbuoni and R. Gatto, Phys. Lett. **B464**, 111 (1999), [hep-ph/9908227](#).
 - [8] D.T. Son and M.A. Stephanov, [hep-ph/9910491](#).
 - [9] M. Rho, A. Wirzba and I. Zahed, Phys. Lett. **B473**, 126 (2000), [hep-ph/9910550](#).
 - [10] R.D. Pisarski and D.H. Rischke, Phys. Rev. **D60**, 094013 (1999), [nucl-th/9903023](#).
 - [11] R.D. Pisarski and D.H. Rischke, [nucl-th/9907041](#).
 - [12] B.Y. Park, M. Rho, A. Wirzba and I. Zahed, [hep-ph/9910347](#).
 - [13] M. Le Bellac, *Thermal Field Theory* (Cambridge University Press, Cambridge 1996).
 - [14] D.T. Son, Phys. Rev. **D59**, 094019 (1999), [hep-ph/9812287](#).
 - [15] T. Schäfer and F. Wilczek, Phys. Rev. **D60**, 114033 (1999), [hep-ph/9906512](#).
 - [16] R.D. Pisarski and D.H. Rischke, [nucl-th/9910056](#).
 - [17] W. E. Brown, J. T. Liu and H. Ren, [hep-ph/9912409](#).
 - [18] D. K. Hong, T. Lee and D. Min, [hep-ph/9912531](#).
 - [19] H. Georgi, Phys. Rev. Lett. **63**, 1917 (1989); Nucl. Phys. **B331**, 311 (1990).
 - [20] M. Harada and K. Yamawaki, Phys. Rev. Lett. **83**, 3374 (1999), [hep-ph/9906445](#).
 - [21] M. Alford, K. Rajagopal and F. Wilczek, Nucl. Phys. **B537**, 443 (1999), [hep-ph/9804403](#).
 - [22] T. Schäfer and F. Wilczek, Phys. Rev. Lett. **82**, 3956 (1999), [hep-ph/9811473](#).
 - [23] M. Bando, T. Kugo, S. Uehara, K. Yamawaki and T. Yanagida, Phys. Rev. Lett. **54**, 1215 (1985).
 - [24] V. Thorsson and A. Wirzba, Nucl. Phys. **A589**, 633 (1995), [nucl-th/9502003](#).
 - [25] C. Itzykson and J.-B. Zuber, *Quantum Field Theory* (McGraw-Hill, New York, 1980).